Age of Information in Multi-source Updating Systems Powered by Energy Harvesting

Mohamed A. Abd-Elmagid, *Member*, *IEEE*, and Harpreet S. Dhillon, *Senior Member*, *IEEE*

***Abstract*—This paper considers a multi-source updating system in which a transmitter node powered by energy harvesting (EH) sends status updates about multiple sources of information to a destination, where the freshness of status updates is measured in terms of Age of Information (AoI). The status updates of each source and harvested energy packets are assumed to arrive at the transmitter according to independent Poisson processes, and the service time of each status update is assumed to be exponentially distributed. Further, the transmitter can harvest energy only when its server is idle. Unlike most of the existing queueing-theoretic analyses of AoI that focus on characterizing its average when the transmitter has a reliable energy source and is hence not powered by EH (referred henceforth as a non-EH transmitter), our analysis is focused on understanding the distributional properties of AoI in multi-source systems through the characterization of its moment generating function (MGF). In particular, we use the stochastic hybrid systems (SHS) framework to derive closed-form expressions of the average/MGF of AoI under several queueing disciplines at the transmitter, including non-preemptive and source-agnostic/source-aware preemptive in service strategies. The generality of our results is demonstrated by recovering several existing results as special cases.**

***Index Terms*—Age of information, energy harvesting, queueing systems, communication networks, stochastic hybrid systems.**

I. Introduction

A typical model for real-time status update systems consists of a *transmitter node* that generates real-time status updates about some physical process(es) of interest and sends them through a communication network to a *destination node*. Such a model can be used to analyze the performance of a plethora of emerging Internet of Things (IoT)-enabled real-time applications including healthcare, factory automation, autonomous vehicles, and smart homes, to name a few [3]. As a concrete example of healthcare applications, large-scale IoT deployments could be useful in containing pandemics through efficient monitoring and contact/infection tracing [4]. The performance of these applications highly depends upon the freshness of the information status at the destination node about its monitored physical process(es). Because of that, the main design objective of such real-time status update systems is to ensure timely delivery of status updates from the transmitter node to the destination node. To measure the freshness of information at the destination node, the authors of [5] introduced the concept of AoI which accounts for the generation time of each status update (which was ignored by conventional performance metrics, specifically throughput and delay). In particular, for a queuing-theoretic model in which status updates are generated at the transmitter node according to a Poisson process, AoI was defined in [5] as the time elapsed since the latest successfully received status update at the destination node was generated at the transmitter node.

As will be discussed next in detail, the queueing-theoretic analyses of AoI have mostly been focused on the characterization of its average in the case of having a non-EH transmitter. However, it is infeasible to ensure the availability of a reliable energy source at the transmitter node in many practical IoT scenarios. For instance, a transmitter node could represent an aggregator deployed at a hard-to-reach place in a large-scale IoT network, where it is impractical to replace or recharge the energy battery at the aggregator [6]. To enable a sustainable operation of real-time status update systems in such scenarios, EH has been considered as a promising solution for powering the transmitter nodes. While there are a handful of prior works analyzing AoI for the system in which a transmitter node is powered by EH, their analyses have been limited to the evaluation of its average and that too in the special case where the transmitter has a single source that generates status updates about a single physical process. Motivated by this, we provide the first queueing-theoretic analysis of the distributional properties of AoI for a generic setup in which an EH-powered transmitter has multiple sources which generate status updates about multiple physical processes.

A. Related Work

For systems in which a non-EH transmitter has a single source that generates status updates about some physical process, referred to as single-source systems, the authors of [5] first derived a closed-form expression of the average AoI under first-come-first-served (FCFS) queueing discipline. The average of AoI or peak AoI (an AoI-related metric introduced in [7] to capture the peak values of AoI over time) is then characterized under several queueing disciplines in a series of subsequent prior works [7]–[13]. Further, a handful of recent works aimed to characterize the distribution (or some distributional properties) of AoI/peak AoI [14]–[19]. While AoI has been extensively analyzed in single-source systems, the prior work on the analysis of AoI in multi-source systems has been fairly limited [20]–[29]. Note that a multi-source system refers to the setup where a non-EH transmitter has multiple sources

M. A. Abd-Elmagid and H. S. Dhillon are with Wireless@VT, Department of ECE, Virginia Tech, Blacksburg, VA. Email: {maelaziz, hdhillon}@vt.edu. The support of the U.S. NSF (Grants CPS-1739642 and CNS-1814477) is gratefully acknowledged. This work will be presented in part at the IEEE ICC 2022 [1] and the IEEE INFOCOM AoI Workshop [2].

This paper has supplementary downloadable material available at http://ieeexplore.ieee.org., provided by the author. The material includes Appendices for proofs referenced in the paper. Contact maelaziz@vt.edu for further questions about this work.

generating status updates about multiple physical processes. The average AoI was characterized for the M/M/1 FCFS queueing model in [20], the M/G/1 FCFS queueing model in [21], and the M/M/1 FCFS with preemption in waiting queueing model (where the transmitter has a buffer that only keeps the latest generated status update from each source) in [22]. The authors of [23] and [24] analyzed the average AoI under scheduled and random multiaccess strategies for delivering the status updates generated from different sources at the transmitter. The average peak AoI was derived for the M/G/1 last-come-first-served (LCFS) queueing model with (without) preemption in service in [25] (in [26]), and for the priority FCFS and LCFS queueing models (where the sources of information are prioritized at the transmitter) in [27]. Further, the distributions of AoI and PAoI were numerically characterized for various discrete time queues in [28], and for a probabilistically preemptive queueing model in [29] where a new arriving status update preempts the one in service with some probability. Different from [7]–[29], our focus in this paper is on the analytical characterization of distributional properties of AoI in the case where the transmitter has multiple sources of information and is powered by EH.

The analyses of the above works were mainly based on identifying the properties of the AoI sample functions and applying geometric arguments, which often involve convoluted calculations of joint moments. This has motivated the authors of [30] and [31] to build on the SHS framework[1] in [32], and derive promising results allowing the use of the SHS approach for the queueing-theoretic analyses of AoI. Following [30], [31], the SHS approach was then used to evaluate the average AoI for a variety of queueing disciplines in [33]–[35], and the MGF of AoI for a two-source system with status update management in [36]. Compared to the analyses of [33]–[36] that considered a non-EH transmitter, the analysis of AoI using the SHS approach becomes much more challenging when we consider an EH-powered transmitter. This is due to the fact that the joint evolution of the battery state at the transmitter and the system occupancy with respect to the status updates has to be incorporated in the process of decision-making (i.e., the decisions of discarding or serving the new arriving status updates at the transmitter). This, in turn, requires analyzing a two-dimensional continuous-time Markov chain (modeling the system discrete state that is represented by the number of energy packets in the battery and the number of status updates in the system) with new transitions associated with the events of harvested energy packet arrivals/departures, compared to the conventional one-dimensional Markov chain used in [33]–[36] to track the number of status updates in a system with a non-EH transmitter.

For the case where the transmitter is powered by EH, there are a handful of prior works [37]–[41] analyzing AoI by applying geometric arguments [37], [38], and by using the SHS approach [39]–[41]. However, the analyses of [37]–[40] have been limited to the evaluation of the average AoI in single-source systems, and the analysis of [41] was focused on the characterization of the distributional properties of AoI in single-source systems. Different from these, this paper makes the first attempt at deriving the distributional properties of AoI for a variety of queueing disciplines in multi-source systems with an EH-powered transmitter. Table I further highlights the gap in the literature that we aim to fill in this paper. Before going into more details about our contributions, it is instructive to note that besides the above queueing theory-based analyses of AoI, there have also been efforts to optimize AoI or some other AoI-related metrics in different communication systems that deal with time critical information (see [42] for a comprehensive survey). For instance, AoI has been studied in the context of EH systems [43]–[54], age-optimal transmission scheduling policies [55]–[57], remote estimation [58], ultra-reliable low-latency vehicular networks [59], unmanned aerial vehicle (UAV)-assisted communication systems [60]–[62], large-scale analysis of IoT networks [63]–[65], cache updating systems [66]–[68], and timely communication in federated learning [69], [70].

[1]A detailed description of the SHS will be provided in Section III.

B. Contributions

This paper analyzes the AoI performance of a multi-source status update system in which an EH-powered transmitter is equipped with a battery of finite capacity to store the harvested energy packets. In particular, we characterize the AoI performance under the LCFS without (LCFS-WP) and with [source-agnostic (LCFS-PS)/source-aware (LCFS-SA)] preemption in service queueing disciplines. An arriving status update at the transmitter preempts the one being served (regardless of its generating source index) under the LCFS-PS queueing discipline, whereas the preemption in service under the LCFS-SA queueing discipline only occurs when the two status updates (the arriving one and the one being served) are generated from the same source. In our analysis, the harvested energy packets/status updates generated from each source are assumed to arrive at the transmitter according to a Poisson process, and the service time of each status update is assumed to be exponentially distributed. For this setup, our main contributions are listed next.

Analysis of the average/MGF of AoI associated with each source at the destination. We use the SHS framework to first derive closed-form expressions of the average AoI of each source for each of the considered queueing disciplines. We then extend our analysis to understand the distributional properties of AoI through the characterization of its MGF under each queuing discipline. The novelty of our analysis lies in the fact that this paper presents the first queueing-theoretic analysis of AoI in multi-source updating systems with an EH-powered transmitter. Further, it is worth noting that the prior analyses of AoI under the source-aware preemptive policies have been limited to the special case where a non-EH transmitter only consists of two sources of information [34]. This, in turn, indicates that our paper is also the first to analyze the AoI performance under a source-aware preemptive in service queueing discipline for the generic case where the transmitter has an arbitrary number of sources. Our results allow us to gain useful insights about the achievable AoI performance by each of the considered queueing disciplines. For instance, we

TABLE I
A SUMMARY OF THE QUEUEING THEORY-BASED ANALYSES OF AOI IN THE EXISTING LITERATURE.

	A non-EH transmitter		EH-powered transmitter	
	Single-source	Multi-source	Single-source	Multi-source
Average of AoI/peak AoI	[5], [7]–[13]	[20]–[27], [30], [33]–[35]	[37]–[40]	This paper
Distribution/distributional properties of AoI/peak AoI	[14]–[19]	[28], [29], [31], [36]	[41]	This paper

analytically characterize the differences between the achievable average AoI performances by the considered queueing disciplines as functions of the system parameters. Further, using the MGF of AoI expressions, we also characterize the relationship between the achievable second moments of AoI by the considered queueing disciplines.

Asymptotic results demonstrating the generality of the derived expressions. We demonstrate that as the aggregate generating rate of status updates from all the sources other than the source of interest approaches zero, the average AoI expressions derived in this paper reduce to their counterparts in [39] and [41] for single-source systems with an EH-powered transmitter, and the derived MGF of AoI expressions reduce to their counterparts in [41]. We further demonstrate that as the arrival rate of harvested energy packets at the transmitter node becomes large, the derived AoI results converge to their counterparts in [7] and [30] for single-source and multi-source systems with a non-EH transmitter, respectively.

System design insights. Our numerical results provide several useful system design insights. For instance, they show that the achievable AoI performance by each queueing discipline improves with the increase in either the battery capacity or the arrival rate of harvested energy packets at the transmitter. They also show that the superiority of the LCFS-PS queueing discipline over the LCFS-WP and LCFS-SA queueing disciplines in terms of the achievable AoI performance (under the exponential service time assumption) comes at the expense of having unfair achievable average AoI values among different sources. Further, they reveal that as the number of sources increases, the LCFS-SA queueing discipline becomes more effective (compared to the LCFS-PS) in achieving fairness between the achievable AoI performances by different sources. Finally, the results demonstrate the importance of incorporating the higher moments of AoI in the implementation/optimization of multi-source real-time status updates systems.

II. SYSTEM MODEL

A. Network Model

We consider a real-time status update system in which an EH-powered transmitter node observes N physical processes, and sends its measurements to a destination node in the form of status update packets. As shown in Fig. 1, the transmitter node contains N sources and a single server; each source generates status updates about one physical process, and the server delivers the status updates generated from all the sources to the destination. In particular, each status update packet generated by source i carries some information about the value of the i-th physical process and a time stamp indicating the time at which that information was measured. This system setup can be mapped to many scenarios of practical interest, such as an IoT network in which an aggregator (represents the transmitter in our model) delivers measurements sensed/generated by the N IoT devices (represent the sources) in its vicinity to a destination node.

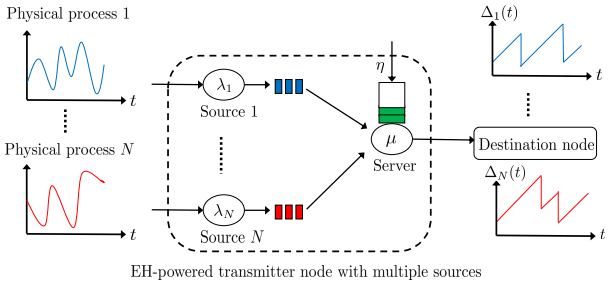

Fig. 1. An illustration of the system setup.

Status update packets generated by the i-th source are assumed to follow a Poisson process with rate λ_i. Further, the energy packets are assumed to arrive at the transmitter according to a Poisson process with rate η, and are stored in a battery queue of length B packets at the server (for serving the update packets generated by the different sources). We consider that each energy packet contains the energy required for sending one status update from any of the sources [37]–[40], and hence the length of the energy battery queue reduces by one whenever a status update is successfully received at the destination. Given that the transmitter node has at least one energy packet in its battery queue, the time needed by its server to send a status update packet is assumed to be a rate μ exponential random variable [5], [7], [8]. Let $\rho = \frac{\lambda}{\mu}$ and $\beta = \frac{\eta}{\mu}$ respectively denote the server utilization and energy utilization factors, where $\lambda = \sum_{i=1}^{N} \lambda_i$. Further, we have $\rho_i = \frac{\lambda_i}{\mu}$, $\lambda_{-i} = \sum_{j=1,\, j\neq i}^{N} \lambda_j$, and $\rho_{-i} = \frac{\lambda_{-i}}{\mu}$.

We quantify the freshness of information status about each physical process at the destination node (as a consequence of receiving status update packets from the transmitter node) using the concept of AoI. Formally, AoI is defined as follows [5].

Definition 1. *Let $t_{i,k}$ and $t'_{i,k}$ denote the arrival and reception time instants of the k-th update packet of source i at the transmitter and destination, respectively. Further, define $L_i(t)$ to be the index of the source i's latest update packet received at the destination by time t, i.e., $L_i(t) = \max\{k|t'_{i,k} \leq t\}$. Then, the AoI associated with the physical process observed by source i at the destination (referred henceforth as AoI of source i) is defined as the following random process*

$$\Delta_i(t) = t - t_{i,L_i(t)}. \tag{1}$$

B. Queueing Disciplines Considered in this Paper

For the above system setup, we analyze the AoI performance at the destination under three different queueing disciplines for managing update packet arrivals at the transmitter node. These queueing disciplines are described next.

- *LCFS-WP queueing discipline*: Under this queueing discipline, a new arriving update packet at the transmitter (from any of the sources) enters service upon its arrival if the server is idle (i.e., there are no status update packets in the system) and the battery contains at least one energy packet; otherwise, the new arriving update packet is discarded.
- *LCFS-PS queueing discipline*: When the server is idle, the management of a new arriving update packet under this queueing discipline is similar to the LCFS-WP one. However, when the server is busy, a new arriving update packet replaces the current packet being served and the old packet in service is discarded.
- *LCFS-SA queueing discipline*: This queueing discipline is similar to the LCFS-PS one with the only difference that a new arriving update packet preempts the packet in service only if the two packets (the new arriving packet and the one in service) are generated from the same source.

Note that the arriving status updates at the transmitter when the battery is empty are discarded to guarantee that a transmitted status update to the destination is always fresh when it starts its service time (its age at this moment is actually 0), which eventually improves the achievable AoI performance. This assumption has also been made in some other closely-related prior works, such as [39] and [40]. Further, according to the LCFS-PS queueing discipline, status updates of a source i with a small λ_i are more likely to be preempted in service by status updates of a source j with $\lambda_j \gg \lambda_i$. Since this issue is resolved under the LCFS-SA queueing discipline by only allowing preemption in service between the status updates generated from the same source, we expect that the LCFS-SA queueing discipline will be more effective (compared to the LCFS-PS) in achieving fairness between the achievable AoI performances by different sources (as will be demonstrated in Section VI). With regards to the EH process, we consider that the transmitter can harvest energy only if its server is idle[2]. This case corresponds to the scenario where the transmitter is equipped with a single radio frequency (RF) chain, and thus can either transmit a status update or harvest energy at a certain time instant.

III. Problem Statement and Solution Approach

Our goal is to analytically characterize the AoI performance of each source at the destination node as a function of: i) the rates of generating status update packets by the N sources $\{\lambda_i\}$, ii) the rate of harvesting energy packets η, iii) the rate of serving status update packets μ, and iv) the finite capacity of the energy battery queue B, at the transmitter node. Unlike most of the analyses of AoI in the existing literature which were focused on deriving its average, our analysis is focused on deriving distributional properties of AoI through the characterization of its MGF. To derive the MGF of AoI for the considered queueing disciplines at the transmitter node (presented in Subsection II-B), we resort to the SHS framework in [32], which was first tailored for the analysis of AoI by [30] and [31]. In the following, we provide a very brief[3] introduction of the SHS framework, which will be useful in understanding our AoI MGF analysis in the subsequent sections. The SHS technique is used to analyze hybrid queueing systems that can be modeled by a combination of discrete and continuous state parameters. In particular, the SHS technique models the discrete state of the system $q(t) \in \mathcal{Q} = \{1, \cdots, m\}$ by a continuous-time finite-state Markov chain, where $\mathcal{Q}$ is the discrete state space. This continuous-time Markov chain governs the dynamics of the system discrete state that usually describes the occupancy of the system, e.g., $q(t)$ represents the numbers of status update and energy packets in the system for our problem. On the other hand, the evolution of the continuous state of the system is described by a continuous process $\mathbf{x}(t) = [x_0(t), \cdots, x_n(t)] \in \mathbb{R}^{1\times(n+1)}$, e.g., $x(t)$ models the evolution of the age-related processes in our system setting.

A transition $l \in \mathcal{L}$ from state q_l to state q'_l (in the Markov chain modeling $q(t)$) occurs due to the arrival of a status update/energy packet or the delivery of a status update to the destination (i.e., the departure of a status update from the system), where $\mathcal{L}$ denotes the set of all transitions. Since the time elapsed between arrivals/departures is exponentially distributed, a transition l takes place with a rate $\lambda^{(l)}\delta_{q_l,q(t)}$, where the Kronecker delta function $\delta_{q_l,q(t)}$ ensures that l occurs only when the discrete state $q(t)$ is equal to q_l. As a consequence of the occurrence of transition l, the discrete state of the system moves from state q_l to state q'_l, and the continuous state $\mathbf{x}$ is reset to $\mathbf{x}'$ according to a binary reset map matrix $\mathbf{A}_l \in \mathbb{B}^{(n+1)\times(n+1)}$ as $\mathbf{x}' = \mathbf{x}\mathbf{A}_l$. Further, $\dot{\mathbf{x}}(t) \triangleq \dfrac{\partial \mathbf{x}(t)}{\partial t} = \mathbf{1}$ holds as long as the state $q(t)$ is unchanged, where $\mathbf{1}$ is the row vector $[1, \cdots, 1] \in \mathbb{R}^{1\times(n+1)}$. Different from ordinary continuous-time Markov chains, an inherent feature of SHSs is the possibility of having self-transitions in the Markov chain modeling the system discrete state. In particular, although a self-transition keeps $q(t)$ unchanged, it causes a change in the continuous process $x(t)$. Further, there may be multiple transitions between any two states in $\mathcal{Q}$ such that their associated reset map matrices are different.

Now, we define some useful quantities for the characterization of the MGF of AoI at the destination node using the SHS technique. Denote by $\pi_q(t)$ the probability of being in state q of the continuous-time Markov chain at time t. Further, let $\mathbf{v}_q(t) = [v_{q0}(t), \cdots, v_{qn}(t)] \in \mathbb{R}^{1\times(n+1)}$ denote the correlation vector between $q(t)$ and $x(t)$, and $\mathbf{v}^s_q(t) = [v^s_{q0}(t), \cdots, v^s_{qn}(t)] \in \mathbb{R}^{1\times(n+1)}$ denote the correlation vector between $q(t)$ and the exponential function $e^{s\mathbf{x}(t)}$, where $s \in \mathbb{R}$.

[2]The case where the transmitter can harvest energy anytime (i.e., even its server is busy) is left as a promising direction of future work.

[3]Interested readers are advised to refer to [30] and [31] for a detailed discussion about the SHS-based analysis of AoI.

Thus, we can respectively express $\pi_q(t)$, $\mathbf{v}_q(t)$ and $\mathbf{v}_q^s(t)$ as

$$\pi_q(t) = \Pr\left(q(t) = q\right) = \mathbb{E}[\delta_{q,q(t)}],\ \forall q \in \mathcal{Q}, \tag{2}$$

$$\mathbf{v}_q(t) = [v_{q0}(t), \cdots, v_{qn}(t)] = \mathbb{E}[\mathbf{x}(t)\delta_{q,q(t)}],\ \forall q \in \mathcal{Q}, \tag{3}$$

$$\mathbf{v}_q^s(t) = [v_{q0}^s(t), \cdots, v_{qn}^s(t)] = \mathbb{E}[e^{s\mathbf{x}(t)}\delta_{q,q(t)}],\ \forall q \in \mathcal{Q}. \tag{4}$$

According to the ergodicity assumption of the continuous-time Markov chain modeling $q(t)$ in the AoI analysis [30], [31], the state probability vector $\pi(t) = [\pi_0(t), \cdots, \pi_m(t)]$ converges uniquely to the stationary vector $\bar{\pi} = [\bar{\pi}_0, \cdots, \bar{\pi}_m]$ satisfying

$$\bar{\pi}_q \sum_{l \in \mathcal{L}_q} \lambda^{(l)} = \sum_{l \in \mathcal{L}'_q} \lambda^{(l)} \bar{\pi}_{q_l},\ q \in \mathcal{Q},\ \sum_{q \in \mathcal{Q}} \bar{\pi}_q = 1, \tag{5}$$

where $\mathcal{L}'_q = \{l \in \mathcal{L} : q'_l = q\}$ and $\mathcal{L}_q = \{l \in \mathcal{L} : q_l = q\}$ denote the sets of incoming and outgoing transitions for state $q, \forall q \in \mathcal{Q}$.

Using the above notations, it has been shown in [31, Theorem 1] that under the ergodicity assumption of the Markov chain modeling $q(t)$, if we can find a non-negative limit $\bar{\mathbf{v}}_q = [\bar{v}_{q0}, \cdots, \bar{v}_{qn}]$, $\forall q \in \mathcal{Q}$, for the correlation vector $\mathbf{v}_q(t)$ satisfying

$$\bar{\mathbf{v}}_q \sum_{l \in \mathcal{L}_q} \lambda^{(l)} = \bar{\pi}_q \mathbf{1} + \sum_{l \in \mathcal{L}'_q} \lambda^{(l)} \bar{\mathbf{v}}_{q_l} \mathbf{A}_l,\ q \in \mathcal{Q}, \tag{6}$$

then:

- The expectation of $x(t)$, $\mathbb{E}[x(t)]$, converges to the following stationary vector:

$$\mathbb{E}[x] = \sum_{q \in \mathcal{Q}} \bar{\mathbf{v}}_q. \tag{7}$$

- There exists $s_0 > 0$ such that for all $s < s_0$, $\mathbf{v}_q^s(t)$ converges to $\bar{\mathbf{v}}_q^s$ that satisfies

$$\bar{\mathbf{v}}_q^s \sum_{l \in \mathcal{L}_q} \lambda^{(l)} = s\bar{\mathbf{v}}_q^s + \sum_{l \in \mathcal{L}'_q} \lambda^{(l)} [\bar{\mathbf{v}}_{q_l}^s \mathbf{A}_l + \bar{\pi}_{q_l} \mathbf{1}\hat{\mathbf{A}}_l],\ q \in \mathcal{Q}, \tag{8}$$

  where $\hat{\mathbf{A}}_l \in \mathbb{B}^{(n+1)\times(n+1)}$ is a binary matrix whose elements are constructed as: $\hat{\mathbf{A}}_l(k,j) = 1$ if $k = j$ and the j-th column of $\mathbf{A}_l$ is a zero vector; otherwise, $\hat{\mathbf{A}}_l(k,j) = 0$. Further, the MGF of the state $\mathbf{x}(t)$, which can be obtained as $\mathbb{E}[e^{s\mathbf{x}(t)}]$, converges to the following stationary vector:

$$\mathbb{E}[e^{s\mathbf{x}}] = \sum_{q \in \mathcal{Q}} \bar{\mathbf{v}}_q^s. \tag{9}$$

From (7) and (9), when the first element of the continuous state $\mathbf{x}(t)$ represents the AoI at the destination node, the expectation and the MGF of AoI at the destination node respectively converge to:

$$\Delta_1 = \sum_{q \in \mathcal{Q}} \bar{v}_{q0}, \tag{10}$$

$$M(s) = \sum_{q \in \mathcal{Q}} \bar{v}_{q0}^s. \tag{11}$$

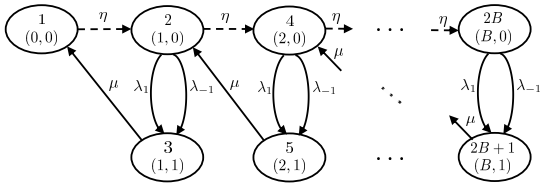

Fig. 2. The Markov chain modeling the discrete state in the LCFS-WP queueing discipline.

IV. The Average AoI for the Considered Queueing Disciplines

It is clear from [31, Theorem 1] (stated in Section III) that in order to use (8) to derive the MGF of AoI at the destination, one needs to find a non-negative limit $\bar{\mathbf{v}}_q$ ($\forall q \in \mathcal{Q}$) satisfying (6), which directly characterizes the average AoI as observed from (7). Thus, we first show in this section that this condition holds for the three queueing disciplines considered in this paper, which will immediately lead to the average AoI characterization for each queueing discipline. Afterwards, we extend our analysis in the next section to derive the AoI MGF.

Without loss of generality, we consider that source 1 is the source of interest in the AoI analysis in the sequel. The AoI performance of the other sources can then be obtained using the same expressions derived for source 1, as will be clear shortly. While analyzing the AoI of source 1, the status update packets associated with the other sources are generated according to a Poisson process with rate $\lambda_{-1} = \sum_{j=2}^{N} \lambda_j$. Using the notations of the SHS approach (presented in Section III), the continuous process $\mathbf{x}(t)$ in each queueing discipline is given by $\mathbf{x}(t) = [x_0(t), x_1(t)]$, where $x_0(t)$ represents the value of the source 1's AoI at the destination node at time instant t (i.e., $\Delta_1(t)$), and $x_1(t)$ indicates the value that the source 1's AoI at the destination will become if the existing update packet in the system completes its service at time instant t (i.e., the packet is delivered to the destination at t). Recall from Section III that as long as there is no change (due to the arrival/departure of an update/energy packet) in the discrete state $q(t)$, we have $\dfrac{\partial \mathbf{x}(t)}{\partial t} = 1$, i.e., the elements of the age vector $\mathbf{x}(t)$ increase linearly with time.

A. LCFS-WP Queueing Discipline

The continuous-time Markov chain modeling the discrete state of the system $q(t) \in \mathcal{Q}$ under the LCFS-WP queueing discipline is depicted in Fig. 2. Each state in $\mathcal{Q}$ represents a potential combination of the number of update packets in the system and the number of energy packets in the battery queue at the server. For instance, a state $q = (e_q, u_q)$ indicates that the system has u_q status update packets and the energy battery queue at the server contains e_q energy packets. Note that since the system can have at most one status update packet at any time instant in the LCFS-WP queueing discipline and there is no need to track the source index from which the update packet in service was generated, we have $u_q \in \{0, 1\}$. In particular, $u_q = 0$ indicates that the system is empty and hence the server is idle, and $u_q = 1$ indicates that the server is serving the existing update packet in the system. Since the

battery queue at the server has a capacity of B packets, we have $e_q \in \{0, 1, \cdots, B\}$. We denote the set of states in the $i-$th row of the Markov chain by r_i. Further, Table II presents the set of different transitions $\mathcal{L}$ and their impact on the values of both $q(t)$ and $\mathbf{x}(t)$. Before proceeding into evaluating $\bar{\mathbf{v}}_q$, $\forall q \in \mathcal{Q}$, satisfying (6), we first describe the set of transitions (for $2 \leq k \leq B$) as follows:

- $l = 4k-3$: This subset of transitions takes place between the states of the Markov chain in r_1, corresponding to the time when the system is empty. In particular, a transition from this set of transitions occurs when a new energy packet is harvested by the transmitter. Clearly, since harvesting a new energy packet does not impact the value of $\Delta_1(t)$, we observe that the first element in the updated value of the age vector $\mathbf{x}\mathbf{A}_l$ (as a consequence of this transition) is x_0, i.e., this transition does not induce any change in the source 1's AoI at the destination. Further, since the server is idle in the states of r_1, the second component of $\mathbf{x}(t)$ (quantifying the age of the source 1's packet in service, if any) becomes irrelevant for such set of states. Note that whenever a component of $\mathbf{x}(t)$ is/becomes irrelevant after the occurrence of some transition l, its value in the updated age vector $\mathbf{x}\mathbf{A}_l$ can be set arbitrarily (except for $l = 4k-1$, as will be clear shortly). Following the convention [30], we set the value corresponding to such irrelevant components in the updated age value to 0, and thus we observe that the second component of $\mathbf{x}\mathbf{A}_{4k-3}$ is 0.
- $l = 4k-2$: A transition from this subset of transitions occurs when there is a new arriving update packet of source 1 at the transmitter node. Since the age of this new arriving update packet at the transmitter is 0 and it does not have any impact on $\Delta_1(t)$, we note that the updated age vector $\mathbf{x}\mathbf{A}_{4k-2}$ is set to be $[x_0, 0]$.
- $l = 4k-1$: A transition from this subset of transitions occurs when any of the sources other than source 1 generates a new update packet at the transmitter node. We note that the first component of $\mathbf{x}\mathbf{A}_{4k-1}$ is x_0 since this transition does not have any impact on $\Delta_1(t)$. Further, to ensure that the value of $\Delta_1(t)$ does not change when this new arriving update packet is received by the destination, we set the second component of $\mathbf{x}\mathbf{A}_{4k-1}$ to x_0, i.e., the value of the source 1's AoI at the arrival instant of this new update packet.
- $l = 4k$: This subset of transitions occurs when the update packet in service is delivered to the destination. When the update packet received at the destination belongs to source 1, the AoI of source 1 is reset to its age; otherwise, the AoI of source 1 does not change. Note that the latter case is achieved by setting the second component of $\mathbf{x}\mathbf{A}_{4k-1}$ to x_0. In addition, since the system becomes empty after the occurrence of this transition, the second component of the age vector $\mathbf{x}(t)$ becomes irrelevant, and thus its corresponding value in the updated age vector $\mathbf{x}\mathbf{A}_{4k}$ is 0.

Now, in order to obtain $\bar{\mathbf{v}}_q$ satisfying (6), the steady state probabilities $\{\bar{\pi}_q\}$ and the vector $\bar{\mathbf{v}}_{q_l}\mathbf{A}_l$ (associated with each transition l in $\mathcal{L}$) need to be computed. The calculations of $\bar{\mathbf{v}}_{q_l}\mathbf{A}_l$, $l \in \mathcal{L}$, are listed in Table II, and $\{\bar{\pi}_q\}$ are given by the following proposition.

TABLE II
TRANSITIONS OF THE LCFS-WP QUEUEING DISCIPLINE IN FIG. 2 ($2 \leq k \leq B$).

l	$q_l \to q_l'$	$\lambda^{(l)}$	$\mathbf{x}\mathbf{A}_l$	$\mathbf{A}_l$	$\hat{\mathbf{A}}_l$	$\bar{\mathbf{v}}_{q_l}\mathbf{A}_l$	$\bar{\pi}_{q_l}\mathbf{1}\hat{\mathbf{A}}_l$
1	$1 \to 2$	η	$[x_0, 0]$	$\begin{bmatrix}1&0\\0&0\end{bmatrix}$	$\begin{bmatrix}0&0\\0&1\end{bmatrix}$	$[\bar{v}_{10}, 0]$	$[0, \bar{\pi}_1]$
2	$2 \to 3$	λ_1	$[x_0, 0]$	$\begin{bmatrix}1&0\\0&0\end{bmatrix}$	$\begin{bmatrix}0&0\\0&1\end{bmatrix}$	$[\bar{v}_{20}, 0]$	$[0, \bar{\pi}_2]$
3	$2 \to 3$	λ_{-1}	$[x_0, x_0]$	$\begin{bmatrix}1&1\\0&0\end{bmatrix}$	$\begin{bmatrix}0&0\\0&0\end{bmatrix}$	$[\bar{v}_{20}, \bar{v}_{20}]$	$[0, 0]$
4	$3 \to 1$	μ	$[x_1, 0]$	$\begin{bmatrix}0&0\\1&0\end{bmatrix}$	$\begin{bmatrix}0&0\\0&1\end{bmatrix}$	$[\bar{v}_{31}, 0]$	$[0, \bar{\pi}_3]$
$4k-3$	$2k-2 \to 2k$	η	$[x_0, 0]$	$\begin{bmatrix}1&0\\0&0\end{bmatrix}$	$\begin{bmatrix}0&0\\0&1\end{bmatrix}$	$[\bar{v}_{2k-2,0}, 0]$	$[0, \bar{\pi}_{2k-2}]$
$4k-2$	$2k \to 2k+1$	λ_1	$[x_0, 0]$	$\begin{bmatrix}1&0\\0&0\end{bmatrix}$	$\begin{bmatrix}0&0\\0&1\end{bmatrix}$	$[\bar{v}_{2k,0}, 0]$	$[0, \bar{\pi}_{2k}]$
$4k-1$	$2k \to 2k+1$	λ_{-1}	$[x_0, x_0]$	$\begin{bmatrix}1&1\\0&0\end{bmatrix}$	$\begin{bmatrix}0&0\\0&0\end{bmatrix}$	$[\bar{v}_{2k,0}, \bar{v}_{2k,0}]$	$[0, 0]$
$4k$	$2k+1 \to 2k-2$	μ	$[x_1, 0]$	$\begin{bmatrix}0&0\\1&0\end{bmatrix}$	$\begin{bmatrix}0&0\\0&1\end{bmatrix}$	$[\bar{v}_{2k+1,1}, 0]$	$[0, \bar{\pi}_{2k+1}]$

Proposition 1. *The steady state probabilities $\{\bar{\pi}_q\}$ can be expressed as*

$$\bar{\pi}_{2k} = \left(\frac{\beta}{\rho}\right)^k \bar{\pi}_1, \tag{12}$$

$$\bar{\pi}_{2k+1} = \rho\left(\frac{\beta}{\rho}\right)^k \bar{\pi}_1, \tag{13}$$

where $1 \leq k \leq B$ and $\bar{\pi}_1$ is given by

$$\bar{\pi}_1 = \begin{cases} \dfrac{1}{1+B(1+\rho)}, & \text{if } \rho = \beta, \\ \dfrac{\rho^B(\beta-\rho)}{\rho^B(\beta-\rho)+\beta(1+\rho)(\beta^B-\rho^B)}, & \text{otherwise.} \end{cases} \tag{14}$$

Proof: The expressions in (12)-(14) follow from solving the set of equations in (5). A detailed proof can be found in Appendix A of [41]. ∎

Having the steady state probabilities $\{\bar{\pi}_q\}$ in Proposition 1 and the set of transitions $\mathcal{L}$ in Table II, we are now ready to derive $\bar{\mathbf{v}}_q$ satisfying (6) as well as to characterize the average value of $\Delta_1(t)$ in the following theorem.

Theorem 1. *Under the LCFS-WP queueing discipline, there exists a non-negative limit $\bar{\mathbf{v}}_q, \forall q \in \mathcal{Q}$, satisfying (6) and the average AoI of source 1 is given by*

$$\overset{\text{WP}}{\Delta}_{1,1} = \frac{1+\rho}{\mu\rho_1} + \frac{\sum_{q\in\mathrm{r}_2}\bar{\pi}_q}{\mu} + \frac{\bar{\pi}_1}{c_0\mu\rho_{-1}} + \sum_{j=1}^{B}\frac{\bar{\pi}_{2j}(\mu\rho_{-1})^{j-1}}{\prod_{h=0}^{j}c_{2h}} + \sum_{j=0}^{B-1}\frac{\bar{\pi}_{2j+3}(\mu\rho_{-1})^{j-1}}{\prod_{h=0}^{j}c_{2h}}, \tag{15}$$

where the set $\{c_0, c_2, \cdots, c_{2B}\}$ is defined as

$$c_{2h} = \begin{cases} \lambda, & h = B, \\ \eta\left(1-\dfrac{\lambda_{-1}}{c_{2h+2}}\right)+\lambda, & 1 \leq h \leq B-1, \\ \eta\left(\dfrac{1}{\lambda_{-1}}-\dfrac{1}{c_2}\right), & h = 0. \end{cases} \tag{16}$$

Proof: See Appendix A. ∎

Note that the average AoI performance for source $i \in \{2,3,\cdots,N\}$ can be obtained directly using (15) by replacing λ_1 with λ_i (which results in replacing $\{\lambda_{-1},\rho_1,\rho_{-1}\}$ with $\{\lambda_{-i},\rho_i,\rho_{-i}\}$ as well). This argument applies to all the results derived in this paper for source 1.

Corollary 1. *For the single source case where $\rho_{-1}=0$ and $\rho=\rho_1$, $\overset{\text{WP}}{\Delta}_{1,1}$ in (15) reduces to*

$$\overset{\text{WP}}{\Delta}_{1,1}=\begin{cases}\dfrac{2B\rho^2+2\left(1+B\right)\rho+B+2}{\mu\left[B\rho^2+(1+B)\rho\right]}, & \text{if } \rho=\beta,\\ \dfrac{\beta^{B+2}\left(2\rho^2+2\rho+1\right)-\rho^{B+2}\left(2\beta^2+2\beta+1\right)}{\mu\left[\beta^{B+2}\left(\rho^2+\rho\right)-\rho^{B+2}\left(\beta^2+\beta\right)\right]}, \end{cases} \tag{17}$$

where the second case in (17) holds when $\rho\neq\beta$. Note that the expression of $\overset{\text{WP}}{\Delta}_{1,1}$ in (17) is identical to the average AoI expression derived in [39, Theorem 3] under the LCFS-WP queueing discipline (for the case of having an EH-powered transmitter with a single source).

Proof: We note from (16) that when $\rho_{-1}=0$, we have $c_{2h}=\eta+\lambda, 1\leq h\leq B-1$, and $c_0=\infty$. Thus, $\overset{\text{WP}}{\Delta}_{1,1}$ in (15) reduces to: $\overset{\text{WP}}{\Delta}_{1,1}=\dfrac{1+\rho}{\mu\rho_1}+\dfrac{\sum_{q\in\mathrm{r}_2}\bar{\pi}_q}{\mu}+\dfrac{\bar{\pi}_1+\bar{\pi}_3}{\eta}$. The final expression in (17) can be obtained by substituting $\{\bar{\pi}_q\}$ from Proposition 1, followed by some algebraic simplifications. ∎

Corollary 2. *When $\beta\to\infty$, $\overset{\text{WP}}{\Delta}_{1,1}$ in (15) reduces to*

$$\lim_{\beta\to\infty}\overset{\text{WP}}{\Delta}_{1,1}=\frac{1+\rho}{\mu\rho_1}+\frac{\rho}{\mu\left(1+\rho\right)}. \tag{18}$$

Note that the expression in (18) is identical to the average AoI expression in the case where a non-EH transmitter with multiple sources employs the LCFS-WP queueing discipline. Further, by setting ρ_1 in (18) to ρ, we obtain $\lim_{\beta\to\infty}\overset{\text{WP}}{\Delta}_{1,1}=\dfrac{2\rho^2+2\rho+1}{\mu\left(\rho^2+\rho\right)}$, which is the average AoI expression derived in [7] for the M/M/1/1 case (where a non-EH transmitter with single source employing the LCFS-WP queueing discipline was considered).

Proof: The result follows from noting that: $\lim_{\beta\to\infty}\dfrac{\bar{\pi}_1}{c_0\mu\rho_{-1}}=\lim_{\beta\to\infty}\dfrac{\bar{\pi}_{2j}\left(\mu\rho_{-1}\right)^{j-1}}{\prod_{h=0}^{j}c_{2h}}=\lim_{\beta\to\infty}\dfrac{\bar{\pi}_{2j+3}\left(\mu\rho_{-1}\right)^{j-1}}{\prod_{h=0}^{j}c_{2h}}=0$ and $\lim_{\beta\to\infty}\dfrac{\sum_{q\in\mathrm{r}_2}\bar{\pi}_q}{\mu}=\dfrac{\rho}{\mu\left(1+\rho\right)}$. ∎

B. LCFS-PS Queueing Discipline

Fig. 3 depicts the Markov chain representing the discrete state of the system under the LCFS-PS queueing discipline, where the structure of $\mathcal{Q}$ is similar to the one associated with the LCFS-WP queueing discipline. Further, the set of transitions in the LCFS-PS queueing discipline can be constructed using Tables II and III. The subset of transitions in Table III

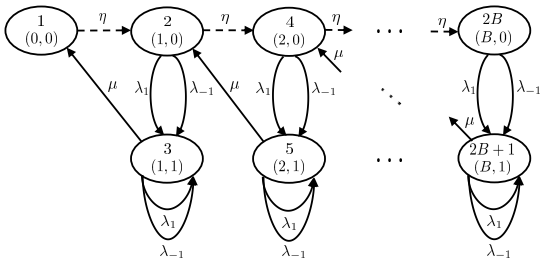

Fig. 3. The Markov chain modeling the discrete state in the LCFS-PS queueing discipline.

refers to the event of having a new arriving update packet at the transmitter node while its server is serving another update packet. According to the mechanism of the LCFS-PS queueing discipline, the status update that is currently being served will be discarded, and the new arrival will enter service upon its arrival. From (5), we note that the self-transitions do not impact the values of the steady state probabilities $\{\bar{\pi}_q\}$, and hence $\{\bar{\pi}_q\}$ in this case can be obtained using Proposition 1. That said, the average value of $\Delta_1(t)$ is provided in the next theorem.

Theorem 2. *Under the LCFS-PS queueing discipline, there exists a non-negative limit $\bar{\mathbf{v}}_q,\forall q\in\mathcal{Q}$, satisfying (6) and the average AoI of source 1 is given by*

$$\overset{\text{PS}}{\Delta}_{1,1}=\frac{1+\rho}{\mu\rho_1}+\frac{\bar{\pi}_1}{c_0\mu\rho_{-1}}+\sum_{j=1}^{B}\frac{\bar{\pi}_{2j}\left(\mu\rho_{-1}\right)^{j-1}}{\prod_{h=0}^{j}c_{2h}}+\frac{1+\rho_{-1}}{1+\rho}\sum_{j=0}^{B-1}\frac{\bar{\pi}_{2j+3}\left(\mu\rho_{-1}\right)^{j-1}}{\prod_{h=0}^{j}c_{2h}}, \tag{19}$$

where the set $\{c_0,c_2,\cdots,c_{2B}\}$ is defined as in (16).

Proof: See Appendix B. ∎

Corollary 3. *For the single source case where $\rho_{-1}=0$ and $\rho=\rho_1$, $\overset{\text{PS}}{\Delta}_{1,1}$ in (19) reduces to: $\overset{\text{PS}}{\Delta}_{1,1}=$*

$$\begin{cases}\dfrac{B\rho^3+(3B+1)\rho^2+(3B+4)\rho+B+2}{\mu\rho\left(1+\rho\right)\left(\rho B+B+1\right)}, & \text{if } \rho=\beta,\\ \dfrac{\beta^{B+2}\left(1+\rho\right)^3-\rho^{B+2}\left[\left(\beta^2+\beta\right)(\rho+2)+1+\rho\right]}{\mu\left(1+\rho\right)\left[\beta^{B+2}\left(\rho^2+\rho\right)-\rho^{B+2}\left(\beta^2+\beta\right)\right]}, \end{cases} \tag{20}$$

where the second case in (20) holds when $\rho\neq\beta$. Note that the expression of $\overset{\text{PS}}{\Delta}_{1,1}$ in (20) is identical to the average AoI expression derived in [41, Corollary 3] under the LCFS-PS queueing discipline (for the case of having an EH-powered transmitter with a single source).

Corollary 4. *When $\beta\to\infty$, $\overset{\text{PS}}{\Delta}_{1,1}$ in (19) reduces to*

$$\lim_{\beta\to\infty}\overset{\text{PS}}{\Delta}_{1,1}=\frac{1+\rho}{\mu\rho_1}. \tag{21}$$

Note that the expression in (21) is identical to the average AoI expression derived in [30, Theorem 2(a)] for the case where a non-EH transmitter with multiple sources employs the LCFS-PS queueing discipline.

TABLE III
TRANSITIONS OF THE LCFS-PS QUEUEING DISCIPLINE IN FIG. 3 ($2 \leq k \leq B$).

l	$q_l \to q_l'$	$\lambda^{(l)}$	$\mathbf{x}\mathbf{A}_l$	$\mathbf{A}_l$	$\hat{\mathbf{A}}_l$	$\bar{\mathbf{v}}_{q_l}\mathbf{A}_l$	$\bar{\pi}_{q_l}\mathbf{1}\hat{\mathbf{A}}_l$
$4B+2k-3$	$2k-1 \to 2k-1$	λ_1	$[x_0, 0]$	$\begin{bmatrix} 1 & 0 \\ 0 & 0 \end{bmatrix}$	$\begin{bmatrix} 0 & 0 \\ 0 & 1 \end{bmatrix}$	$[\bar{v}_{2k-1,0}, 0]$	$[0, \bar{\pi}_{2k-1}]$
$4B+2k-2$	$2k-1 \to 2k-1$	λ_{-1}	$[x_0, x_0]$	$\begin{bmatrix} 1 & 1 \\ 0 & 0 \end{bmatrix}$	$\begin{bmatrix} 0 & 0 \\ 0 & 0 \end{bmatrix}$	$[\bar{v}_{2k-1,0}, \bar{v}_{2k-1,0}]$	$[0, 0]$

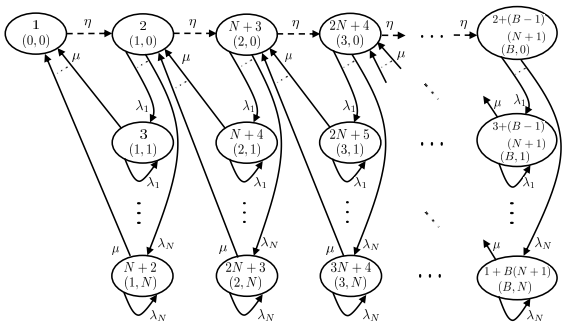

Fig. 4. The Markov chain modeling the discrete state in the LCFS-SA queueing discipline.

Remark 1. *Note that from Theorems 1 and 2, we have*

$$\overset{\text{WP}}{\Delta}_{1,1} - \overset{\text{PS}}{\Delta}_{1,1} = \frac{\sum_{q\in \mathrm{r}_2} \bar{\pi}_q}{\mu} + \frac{\rho_1}{1+\rho} \sum_{j=0}^{B-1} \frac{\bar{\pi}_{2j+3} \left(\mu\rho_{-1}\right)^{j-1}}{\prod_{h=0}^{j} c_{2h}}. \tag{22}$$

Since the set $\{c_0, c_2, \cdots, c_{2B}\}$ contains positive real numbers, we observe from (22) that $\overset{\text{WP}}{\Delta}_{1,1} - \overset{\text{PS}}{\Delta}_{1,1} \geq 0$ for any choice of values of the system parameters. This, in turn, indicates the superiority of the LCFS-PS queueing discipline over LCFS-WP in terms of the achievable average AoI at the destination node.

C. LCFS-SA Queueing Discipline

Under the LCFS-SA queueing discipline, the continuous-time Markov chain modeling the discrete state of the system $q(t) \in \mathcal{Q}$ is depicted in Fig. 4. Recall that according to the mechanism of the LCFS-SA queueing discipline, a new arriving update packet preempts the packet in service only if the two packets are generated from the same source. Thus, the discrete state of the system needs to not only account for the number of update packets in the system (as it was the case for the LCFS-WP and the LCFS-PS queueing disciplines) but also track the index of the source which generated the current packet in service. Because of that, we observe from Fig. 4 that for a state $q = (e_q, u_q)$, we have $u_q \in \{0, 1, \cdots, N\}$. In particular, $u_q = 0$ indicates that the system is empty and hence the server is idle, and $u_q = i$ indicates that there is an update packet in service and the index of its generating source is i. Further, due to the finite capacity of the battery queue at the server, we have $e_q \in \{0, 1, \cdots, B\}$. The set of transitions $\mathcal{L}$ and their impact on the values of both $q(t)$ and $\mathbf{x}(t)$ are presented in Table IV in the supplementary material. We start the analysis by characterizing the steady state probabilities $\{\bar{\pi}_q\}$ in the following proposition.

Proposition 2. *The steady state probabilities $\{\bar{\pi}_q\}$ can be expressed as*

$$\bar{\pi}_{2+(k-1)(N+1)} = \left(\frac{\beta}{\rho}\right)^k \bar{\pi}_1, \tag{23}$$

$$\bar{\pi}_{2+i+(k-1)(N+1)} = \rho_i \left(\frac{\beta}{\rho}\right)^k \bar{\pi}_1, \tag{24}$$

where $1 \leq k \leq B$, $1 \leq i \leq N$, and $\bar{\pi}_1$ is given by (14).

Proof: The expressions in (23) and (24) follow directly from the solution of (5). ∎

Now, using Table IV and Proposition 2, the average AoI is obtained in the following theorem.

Theorem 3. *Under the LCFS-SA queueing discipline, there exists a non-negative limit $\bar{\mathbf{v}}_q, \forall q \in \mathcal{Q}$, satisfying (6) and the average AoI of source 1 is given by: $\overset{\text{SA}}{\Delta}_{1,1} =$*

$$\frac{1+\rho}{\mu\rho_1\left(1+\rho_1\right)} + \frac{\left(1+\rho\right)\sum_{q\in\mathcal{Q}/\mathrm{r}_2}\bar{\pi}_q}{\mu\left(1+\rho_1\right)} + \frac{\sum_{q\in\mathcal{Q}/\mathrm{r}_1}\bar{\pi}_q}{\mu} + \bar{v}_{10}, \tag{25}$$

where $\bar{v}_{10}$ is given by

$$\bar{v}_{10} = \frac{\bar{\pi}_1}{\bar{c}_{-1}\mu\rho_{-1}} + \sum_{j=1}^{B} \frac{\bar{\pi}_{2+(j-1)(N+1)} \left(\mu\rho_{-1}\right)^{j-1}}{\prod_{h=0}^{j} \bar{c}_{h-1}} + \sum_{j=0}^{B-1} \frac{\frac{\bar{\pi}_{3+j(N+1)}}{1+\rho_1} + \sum_{m=4+j(N+1)}^{1+(j+1)(N+1)} \bar{\pi}_m}{\prod_{h=0}^{j} \bar{c}_{h-1}} \left(\mu\rho_{-1}\right)^{j-1}, \tag{26}$$

where the set $\{\bar{c}_{-1}, \bar{c}_0, \cdots, \bar{c}_{B-1}\}$ is defined as

$$\bar{c}_h = \begin{cases} \lambda, & h = B-1, \\ \eta\left(1 - \dfrac{\lambda_{-1}}{\bar{c}_{h+1}}\right) + \lambda, & 0 \leq h \leq B-2, \\ \eta\left(\dfrac{1}{\lambda_{-1}} - \dfrac{1}{\bar{c}_0}\right), & h = -1. \end{cases} \tag{27}$$

Proof: See Appendix D in the supplementary material. ∎

Corollary 5. *Note that for the single source case where $\rho_{-1} = 0$ and $\rho = \rho_1$, the LCFS-PS and LCFS-SA queueing disciplines are similar. Because of that, $\overset{\text{SA}}{\Delta}_{1,1}$ in (25) reduces to (20) when $\rho = \rho_1$. Further, when $\beta \to \infty$, $\overset{\text{SA}}{\Delta}_{1,1}$ in (25) reduces to*

$$\lim_{\beta\to\infty} \overset{\text{SA}}{\Delta}_{1,1} = \frac{1+\rho}{\mu\rho_1} + \frac{\rho_{-1}}{\mu\left(1+\rho\right)\left(1+\rho_1\right)}, \tag{28}$$

which indicates that $\lim_{\beta\to\infty} \overset{\text{PS}}{\Delta}_{1,1} \leq \lim_{\beta\to\infty} \overset{\text{SA}}{\Delta}_{1,1} \leq \lim_{\beta\to\infty} \overset{\text{WP}}{\Delta}_{1,1}$.

Remark 2. *Note that from Theorems 1, 2 and 3, we have*

$$\overset{\text{WP}}{\Delta}_{1,1} - \overset{\text{SA}}{\Delta}_{1,1} = \frac{\rho_1 (1+\rho) \sum_{k=1}^{B} (\frac{\beta}{\rho})^k}{\mu (1+\rho_1) \left[1 + (1+\rho) \sum_{k=1}^{B} \left(\frac{\beta}{\rho}\right)^k\right]} + \frac{\bar{\pi}_1 \rho_1^2}{1+\rho_1} \sum_{j=0}^{B-1} \frac{\left(\frac{\beta}{\rho}\right)^{j+1} (\mu\rho_{-1})^{j-1}}{\prod_{h=0}^{j} \bar{c}_{h-1}}, \quad (29)$$

$$\overset{\text{SA}}{\Delta}_{1,1} - \overset{\text{PS}}{\Delta}_{1,1} = \frac{\rho_{-1} \sum_{k=1}^{B} (\frac{\beta}{\rho})^k}{\mu (1+\rho_1) \left[1 + (1+\rho) \sum_{k=1}^{B} \left(\frac{\beta}{\rho}\right)^k\right]} + \frac{\bar{\pi}_1 \rho_1 \rho_{-1}}{(1+\rho_1)(1+\rho)} \sum_{j=0}^{B-1} \frac{\left(\frac{\beta}{\rho}\right)^{j+1} (\mu\rho_{-1})^{j-1}}{\prod_{h=0}^{j} \bar{c}_{h-1}}. \quad (30)$$

Since the set $\{\bar{c}_{-1}, \bar{c}_0, \cdots, \bar{c}_{B-1}\}$ *contains positive real numbers, we observe from (29) and (30) that* $\overset{\text{PS}}{\Delta}_{1,1} \leq \overset{\text{SA}}{\Delta}_{1,1} \leq \overset{\text{WP}}{\Delta}_{1,1}$ *for any choice of values of the system parameters.*

V. The MGF of AoI for the Considered Queueing Disciplines

This section presents the analysis of the MGF of AoI under each of the queueing disciplines considered in this paper.

A. LCFS-WP Queueing Discipline

According to Theorem 1, there exists a non-negative limit $\bar{\mathbf{v}}_q, \forall q \in \mathcal{Q}$, satisfying (6), under the LCFS-WP queueing discipline. Thus, the MGF of AoI can be evaluated using (8) as in the following theorem, where the calculations required to solve the set of equations (i.e., $\bar{\mathbf{v}}^s_{q_l} \mathbf{A}_l$ and $\bar{\pi}_{q_l} \mathbf{1} \hat{\mathbf{A}}_l$, $l \in \mathcal{L}$) in (8) are listed in Table II.

Theorem 4. *The MGF of AoI of source 1 for the LCFS-WP queueing discipline is given by*

$$\overset{\text{WP}}{M}_1(\bar{s}) = \frac{\rho_1 (1+\rho-\bar{s}) \sum_{q \in \mathrm{r}_1/\{1\}} \bar{\pi}_q + \bar{v}^s_{10} \rho_1 (1-\bar{s})}{(1-\bar{s}) \left[(1-\bar{s})(\rho-\bar{s}) - \rho_{-1}\right]}, \quad (31)$$

where $\bar{s} = \frac{s}{\mu}$ *and* $\bar{v}^s_{10}$ *is given by*

$$\bar{v}^s_{10} = \frac{\rho_1}{\rho_{-1}} \sum_{j=0}^{B-1} \frac{\bar{\pi}_{2j+2}}{\prod_{h=0}^{j} c^s_{2h}} \left(\frac{\mu\rho_{-1}}{1-\bar{s}}\right)^j, \quad (32)$$

where the set $\{c^s_0, c^s_2, \cdots, c^s_{2B}\}$ *is defined as*

$$c^s_{2h} = \begin{cases} \lambda - s, & h = B, \\ \eta + \lambda - s - \dfrac{\mu\eta\lambda_{-1}}{c^s_{2h+2}(\mu - s)}, & 1 \leq h \leq B-1, \\ \dfrac{(\mu-s)(\eta-s)}{\mu\lambda_{-1}} - \dfrac{\eta}{c^s_2}, & h = 0. \end{cases} \quad (33)$$

Proof: See Appendix C. ∎

Corollary 6. *When* $\rho_{-1} = 0$ *(i.e.,* $\rho_1 = \rho$*),* $\overset{\text{WP}}{M}_1(\bar{s})$ *in (31) reduces to the following MGF of AoI derived in [41, Theorem 1] for the case where an EH-powered transmitter with a single source employs the LCFS-WP queueing discipline*

$$\overset{\text{WP}}{M}_1(\bar{s}) = \frac{\rho\bar{\pi}_1 \left[\bar{s}^2\theta - \bar{s}\theta(1+\rho+\beta) + \beta(1+\theta+\theta\rho)\right]}{(1-\bar{s})^2 (\rho-\bar{s})(\beta-\bar{s})}, \quad (34)$$

where θ *can be expressed as*

$$\theta = \begin{cases} B, & \text{if } \rho = \beta, \\ \dfrac{\beta(\beta^B - \rho^B)}{\rho^B(\beta-\rho)}, & \text{otherwise.} \end{cases} \quad (35)$$

Proof: When $\rho_{-1} = 0$, we first note from (33) that we have: $c^s_{2h} = \eta + \lambda - s, 1 \leq h \leq B-1$, and $c^s_0 = \infty$. As a result, $\bar{v}^s_{10}$ reduces to $\dfrac{\rho_1\bar{\pi}_2}{(1-\bar{s})(\beta-\bar{s})}$. The final expression in (34) can be obtained by defining $\sum_{q \in \mathrm{r}_1/\{1\}} \bar{\pi}_q = \theta\bar{\pi}_1$ and substituting $\bar{\pi}_2$ from Proposition 1 as $\frac{\beta}{\rho}\bar{\pi}_1$. ∎

B. LCFS-PS Queueing Discipline

Based on Theorem 2, the MGF of AoI under the LCFS-PS queueing discipline is derived in the following theorem by solving the set of equations in (8) using the calculations in Tables II and III.

Theorem 5. *The MGF of AoI of source 1 for the LCFS-PS queueing discipline is given by*

$$\overset{\text{PS}}{M}_1(\bar{s}) = \frac{\rho_1 (1 - \bar{\pi}_1 + \bar{v}^s_{10})}{(1-\bar{s})(\rho-\bar{s}) - \rho_{-1}}, \quad (36)$$

where $\bar{v}^s_{10}$ *is given by*

$$\bar{v}^s_{10} = \frac{\mu\rho_1}{1+\rho-\bar{s}} \sum_{j=0}^{B-1} \frac{\bar{\pi}_{2j+2} + \bar{\pi}_{2j+3}}{\prod_{h=0}^{j} c^s_{2h}} \left(\frac{\mu\rho_{-1}}{1-\bar{s}}\right)^{j-1}, \quad (37)$$

where the set $\{c^s_0, c^s_2, \cdots, c^s_{2B}\}$ *is defined as in (33).*

Proof: See Appendix E in the supplementary material. ∎

Corollary 7. *When* $\rho_{-1} = 0$ *(i.e.,* $\rho_1 = \rho$*),* $\overset{\text{PS}}{M}_1(\bar{s})$ *in (36) reduces to the following MGF of AoI derived in [41, Theorem 3] for the case where an EH-powered transmitter with a single source employs the LCFS-PS queueing discipline*

$$\overset{\text{PS}}{M}_1(\bar{s}) = \frac{\bar{\pi}_1 \left[\bar{s}^2\theta - \bar{s}\theta(1+\rho+\beta) + \beta(1+\theta+\theta\rho)\right]}{\rho^{-1}(1+\rho)^{-1}(1-\bar{s})(\rho-\bar{s})(1+\rho-\bar{s})(\beta-\bar{s})}, \quad (38)$$

where θ *is given by (35).*

C. LCFS-SA Queueing Discipline

Based on Theorem 3, the MGF of AoI under the LCFS-SA queueing discipline is derived in the following theorem by solving the set of equations in (8) using the calculations in Table IV.

Theorem 6. *The MGF of AoI of source 1 for the LCFS-SA queueing discipline is given by*

$$\overset{\text{SA}}{M}_1(\bar{s}) = \frac{(1+\rho-\bar{s})\sum_{q\in \mathrm{r}_1\cup \mathrm{r}_2/\{1\}}\bar{\pi}_q + (1+\rho_1-\bar{s})\,\bar{v}^s_{10}}{\rho_1^{-1}\,(1+\rho_1-\bar{s})\left[(1-\bar{s})\,(\rho-\bar{s})-\rho_{-1}\right]}, \tag{39}$$

where $\bar{v}^s_{10}$ is given by

$$\bar{v}^s_{10} = \frac{\mu\rho_1}{1+\rho_1-\bar{s}}\sum_{j=0}^{B-1}\frac{\bar{\pi}_{2+j(N+1)}+\bar{\pi}_{3+j(N+1)}}{\prod_{h=0}^{j}\bar{c}^s_{h-1}}\left(\frac{\mu\rho_{-1}}{1-\bar{s}}\right)^{j-1}, \tag{40}$$

where the set $\{\bar{c}^s_{-1},\bar{c}^s_0,\cdots,\bar{c}^s_{B-1}\}$ is defined as

$$\bar{c}^s_h = \begin{cases} \lambda-s, & h=B-1,\\ \eta+\lambda-s-\dfrac{\mu\eta\lambda_{-1}}{\bar{c}^s_{h+1}\,(\mu-s)}, & 0\le h\le B-2,\\ \dfrac{(\mu-s)\,(\eta-s)}{\mu\lambda_{-1}}-\dfrac{\eta}{\bar{c}^s_0}, & h=-1. \end{cases} \tag{41}$$

Proof: See Appendix F in the supplementary material. ■

Corollary 8. *When $\rho_{-1}=0$ (i.e., $\rho_1=\rho$), $\overset{\text{SA}}{M}_1(\bar{s})$ in (39) reduces to the MGF of AoI derived in [41, Theorem 3] (given by (38)) for the case where an EH-powered transmitter with a single source employs the LCFS-PS queueing discipline.*

Remark 3. *Let $\overset{\text{D}}{\Delta}_{i,j}$ denote the j-th moment of source i's AoI under queueing discipline* D*. Similar to Remark 2, one can deduce from Corollaries 9, 10 and 11 (presented in Appendix G in the supplementary material) that $\overset{\text{PS}}{\Delta}_{1,2}\le\overset{\text{SA}}{\Delta}_{1,2}\le\overset{\text{WP}}{\Delta}_{1,2}$ for any choice of values of the system parameters. Further, when $\rho_{-1}=0$ (i.e., $N=1$), we have $\overset{\text{WP}}{\Delta}_{1,2}-\overset{\text{PS}}{\Delta}_{1,2}=\overset{\text{WP}}{\Delta}_{1,2}-\overset{\text{SA}}{\Delta}_{1,2}$.*

The insights obtained in Remarks 1-3 are quite useful from an engineering perspective since they allow one to: i) quantify improvement of one queueing discipline over another in terms of the achievable AoI performance, and ii) specify the ranges of system parameter values over which a certain queueing discipline achieves a better AoI performance than another queueing discipline.

VI. Numerical Results

In this section, we study the impact of the system design parameters on the achievable AoI performance under each of the three queueing disciplines considered in this paper. We use $\mu=1$ in all the figures. In Fig 5, we first verify the accuracy of the analytical expressions of the first and second moments of AoI for all the queueing disciplines (obtained in Corollaries 9, 10 and 11 using the MGFs derived in Theorems 4, 5 and 6) in (a)-(c) by comparing them to their simulated counterparts (obtained numerically using [31, Theorem 1]). We then study the impact of battery capacity B on the achievable pairs of average AoI $(\Delta_{1,1},\Delta_{2,1})$ when $N=2$ and ρ is fixed. We observe from Fig. 5 that the AoI performance of each queueing discipline improves with increasing β until it converges to its counterpart with a non-EH transmitter (as stated in Corollaries 2, 4 and 5). Further, it is interesting to observe that setting B to 20 is sufficient to achieve a similar AoI performance to that of a non EH-powered updating system. This happens since increasing B or β decreases the likelihood that the battery queue is empty upon the arrival of a new status update at the transmitter when the server is idle, and hence increases the likelihood of delivering new arriving updates to the destination.

In Fig. 6, we compare the three queueing disciplines studied in this paper when $N=2$ in terms of: i) the achievable average AoI pairs $(\Delta_{1,1},\Delta_{2,1})$ in Figs. 6a and 6d, ii) the average sum-AoI $\Delta_{1,1}+\Delta_{2,1}$ in Figs. 6b and 6e, and iii) the Jain's fairness index in Figs. 6c and 6f, which is defined as $\text{JFI}=\dfrac{\left(\sum_{i=1}^{N}\Delta_{i,1}\right)^2}{N\sum_{i=1}^{N}\Delta_{i,1}^2}$ [71]. Note that the JFI $\in\left[N^{-1},1\right]$ is a measure of the fairness between the achievable average AoI values by different sources such that JFI $=1$ when the average AoI values of different sources are equal (the best scenario with respect to fairness). First, we observe from Figs. 6a, 6b, 6d and 6e the superiority of the LCFS-PS queueing discipline over the LCFS-WP and the LCFS-SA queueing disciplines in terms of the achievable average AoI performance[4] (which supports our arguments in Remark 2). However as indicated from Figs. 6c and 6f, such a superiority of the LCFS-PS queueing discipline comes at the expense of having unfair achievable average AoI values among different sources. Second, we observe from Figs. 6c and 6f that as N increases, the superiority of the LCFS-SA queueing discipline over LCFS-PS in terms of the achievable fairness performance becomes more significant. As expected, this happens since the LCFS-SA queueing discipline does not allow source-agnostic preemption in service. Finally, as was the case in [41] for single-source systems with an EH-powered transmitter node, we observe from Figs. 6a, 6b, 6d and 6e that the standard deviation of AoI σ associated with each queueing discipline in multi-source systems is relatively large with respect to the average value. This indicates that the implementation of multi-source status update systems based on just the average value of AoI does not ensure reliability, and it is crucial to incorporate the higher moments of AoI in the design of such systems. This insight demonstrates the significance of the analytical distributional properties of AoI derived in this paper.

VII. Conclusion

This paper analytically characterized the AoI performance of multi-source EH updating systems, where an EH-powered transmitter sends status updates about several observed physical processes to a destination. In particular, we used the SHS approach to analyze AoI under non-preemptive and source-agnostic (LCFS-PS)/source-aware (LCFS-SA) preemptive in service queueing disciplines. We started our analysis by characterizing the average AoI for each considered queueing discipline in closed-form. We then extended the analysis

[4]Note that this argument holds under the exponential service time assumption. One possible extension to our work is to investigate the validity of the argument for a general service time distribution.

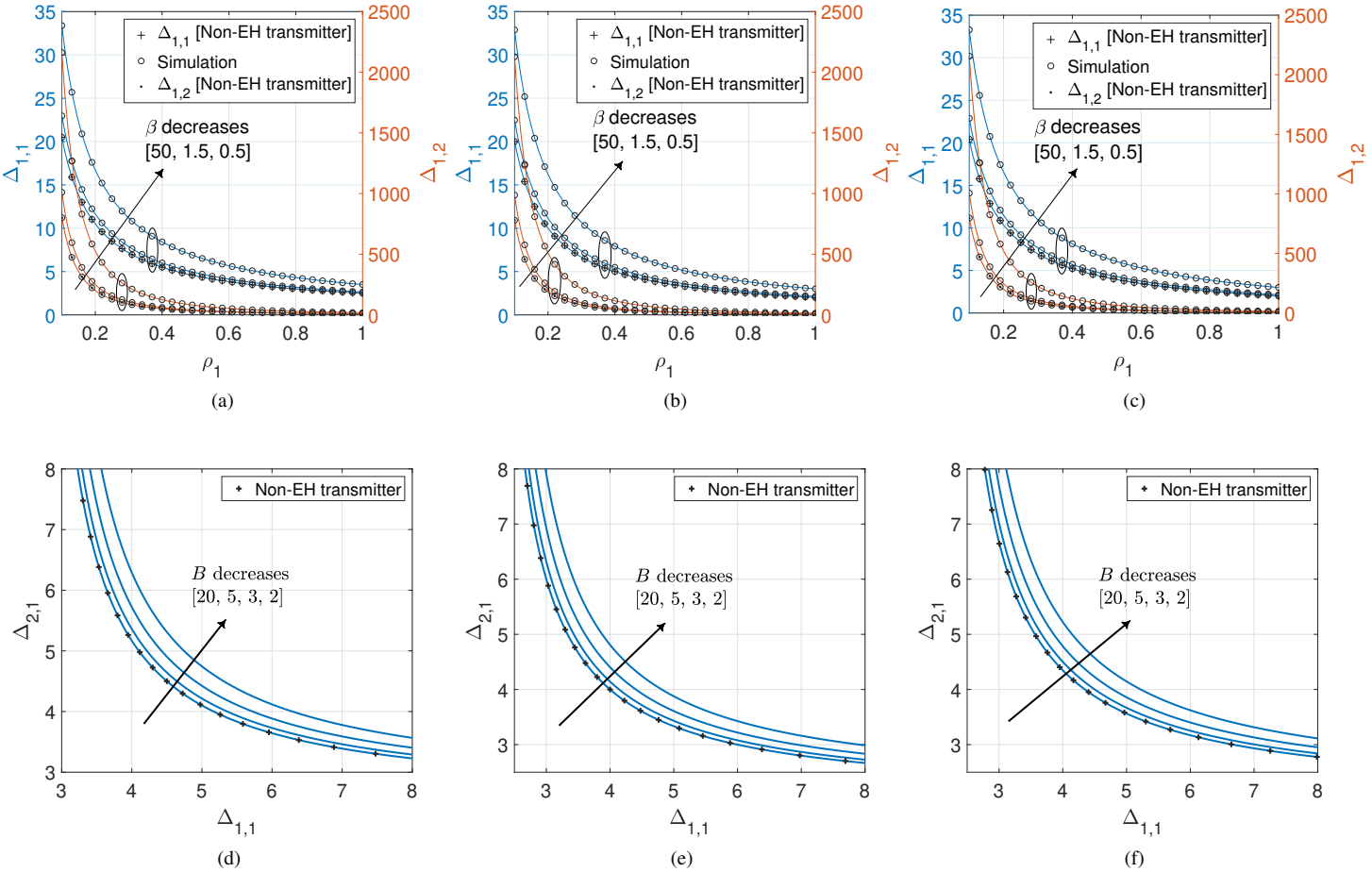

Fig. 5. Verification of the analytical results derived in Corollaries 9, 10 and 11: (a) the LCFS-WP queueing discipline, (b) the LCFS-PS queueing discipline, and (c) the LCFS-SA queueing discipline. In (a)-(c), N can be chosen arbitrary and we use $\rho = 1$. Impact of battery capacity B: (d) the LCFS-WP queueing discipline, (e) the LCFS-PS queueing discipline, and (f) the LCFS-SA queueing discipline. In (d)-(f), we use $N = 2$, $\beta = 1.5$, and $\rho = 1$.

to study the distributional properties of AoI through the characterization of its MGF. Our analytical results allowed us to obtain several useful insights regarding the achievable AoI performance under the considered queueing disciplines. For instance, the differences between the achievable average AoI performances by the considered queueing disciplines were characterized in closed-form as functions of the system parameters. Further, our asymptotic results demonstrated the generality of the derived expressions by recovering several existing results for single source-systems with an EH-powered transmitter (when the aggregate generating rate of status updates from all the sources other than the source of interest approaches zero), and for multi-source systems with a non-EH transmitter (when the arrival rate of harvested energy packets becomes large).

Several key system design insights were also drawn from our numerical results. For instance, our results revealed a fundamental trade-off between obtaining a minimum average sum-AoI and having fair achievable average AoI values among different sources. Further, they showed the effectiveness of the LCFS-SA queueing discipline (compared to the LCFS-PS) in achieving fairness between different sources in term of the achievable AoI performance (especially when the number of sources is large). Finally, the results demonstrated that it is necessary to incorporate the higher moments of AoI in the implementation/optimization of multi-source real-time status updates systems rather than just relying on its average value.

While our focus in this paper was on deriving the marginal AoI distribution of each source under a variety of queuing disciplines, extending our results to characterize the joint distribution of AoI processes associated with different sources is a promising direction of future work. A major technical challenge in such problem is that [31, Theorem 1] is not applicable to the joint performance analysis of AoI processes associated with different sources.

Appendix

A. Proof of Theorem 1

We first show the existence of a non-negative limit $\bar{\mathbf{v}}_q, \forall q \in \mathcal{Q}$, satisfying (6), and then we obtain the average AoI of source 1 using $\overset{\text{WP}}{\Delta}_{1,1} = \sum_{q\in\mathcal{Q}} \bar{v}_{q0}$. The set of equations in (6) can be expressed as

$$q_1: \quad \eta[\bar{v}_{10}, \bar{v}_{11}] = \mu[\bar{v}_{31}, 0] + [\bar{\pi}_1, \bar{\pi}_1], \tag{42}$$

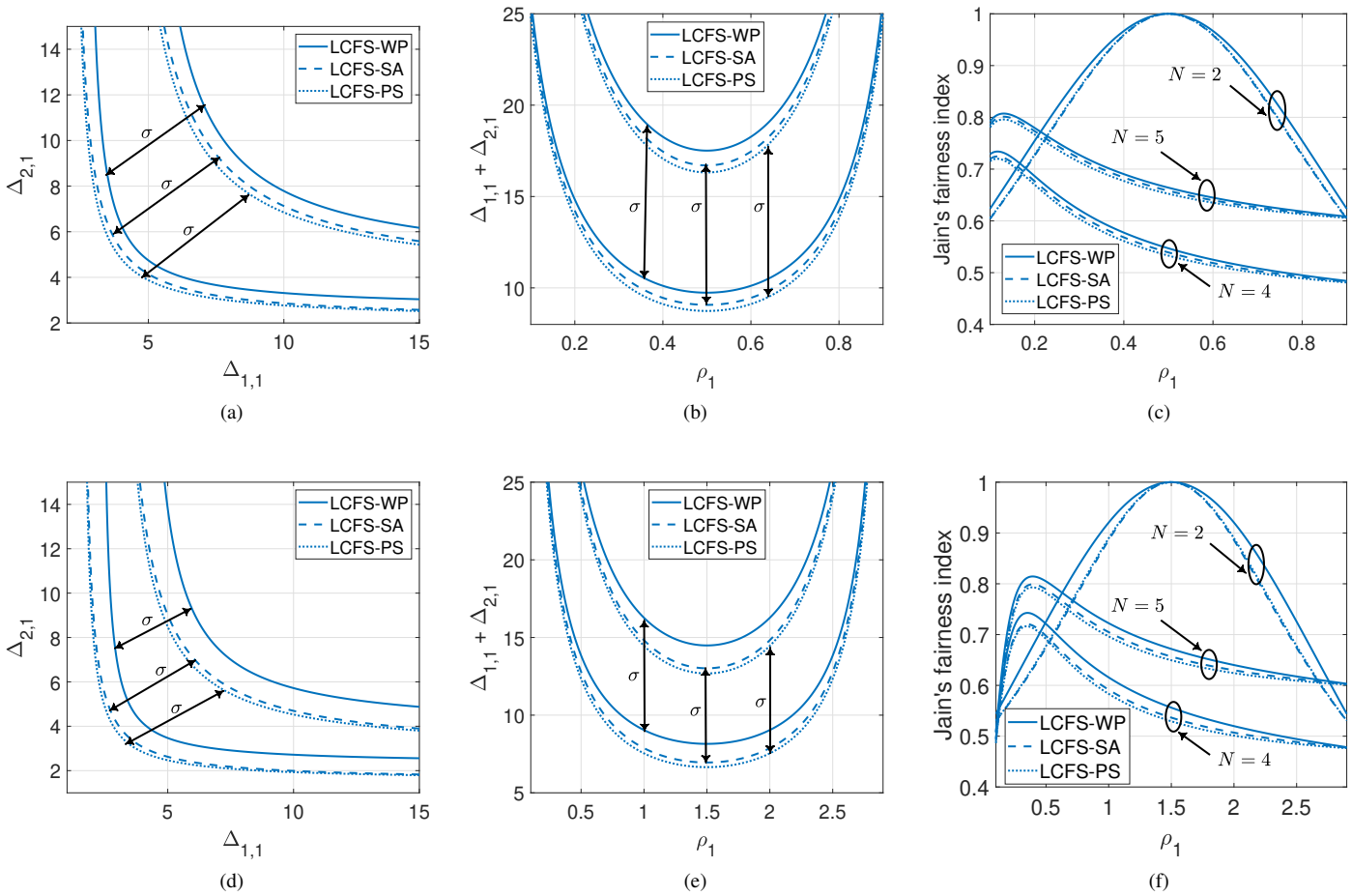

Fig. 6. Comparison between the achievable AoI performance of the queueing disciplines considered in this paper. We use $\beta = 1.5$, $B = 2$, and $\rho = 1$ [$\rho = 3$] in (a), (b) and (c) [(d), (e) and (f)]. Further, we use $N = 2$ in (a), (b), (d) and (e). In (c) and (f) for $N \in \{4, 5\}$, we set $\rho_2 = 0.1(\rho - \rho_1)$ and $\rho_i = \frac{0.9}{N-2}(\rho - \rho_1)$, $3 \le i \le N$.

$$q_2: \quad (\eta+\lambda)\,[\bar{v}_{20}, \bar{v}_{21}] = \mu[\bar{v}_{51}, 0] + \eta[\bar{v}_{10}, 0] + [\bar{\pi}_2, \bar{\pi}_2], \tag{43}$$

$$q_{2k}, 2 \le k \le B-1: \quad (\eta+\lambda)\,[\bar{v}_{2k,0}, \bar{v}_{2k,1}] = \mu[\bar{v}_{2k+3,1}, 0] + \eta[\bar{v}_{2k-2,0}, 0] + [\bar{\pi}_{2k}, \bar{\pi}_{2k}], \tag{44}$$

$$q_{2B}: \quad \lambda[\bar{v}_{2B,0}, \bar{v}_{2B,1}] = \eta[\bar{v}_{2B-2,0}, 0] + [\bar{\pi}_{2B}, \bar{\pi}_{2B}], \tag{45}$$

$$q_{2k+1}, 1 \le k \le B: \quad \mu[\bar{v}_{2k+1,0}, \bar{v}_{2k+1,1}] = [\lambda\bar{v}_{2k,0}, \lambda_{-1}\bar{v}_{2k,0}] + [\bar{\pi}_{2k+1}, \bar{\pi}_{2k+1}]. \tag{46}$$

From (45), $\bar{v}_{2B,0}$ can be expressed as

$$\bar{v}_{2B,0} = \frac{\eta\bar{v}_{2B-2,0}}{c_{2B}} + \frac{\bar{\pi}_{2B}}{c_{2B}}, \tag{47}$$

where $c_{2B} = \lambda$. Substituting $k = B-1$ in (44), $\bar{v}_{2B-2,0}$ can be expressed as

$$\bar{v}_{2B-2,0} = \frac{\eta\bar{v}_{2B-4,0}}{c_{2B-2}} + \frac{\bar{\pi}_{2B-2}}{c_{2B-2}} + \frac{\lambda_{-1}\bar{\pi}_{2B}}{c_{2B-2}c_{2B}} + \frac{\bar{\pi}_{2B+1}}{c_{2B-2}}, \tag{48}$$

where $\bar{v}_{2B+1,1}$ and $\bar{v}_{2B,0}$ were respectively substituted from (46) and (47), and $c_{2B-2} = \eta\left(1 - \frac{\lambda_{-1}}{c_{2B}}\right) + \lambda$. Repeated application of (44) gives

$$\bar{v}_{2k,0} = \frac{\eta\bar{v}_{2k-2}}{c_{2k}} + \sum_{j=1}^{B+1-k} \frac{\bar{\pi}_{2(k+j-1)}\lambda_{-1}^{j-1}}{\prod_{h=1}^{j} c_{2(k+h-1)}} + \sum_{j=1}^{B-k} \frac{\bar{\pi}_{2(k+j-1)+3}\lambda_{-1}^{j-1}}{\prod_{h=1}^{j} c_{2(k+h-1)}}, \; 2 \le k \le B, \tag{49}$$

$$\bar{v}_{20} = \frac{\eta\bar{v}_{10}}{c_2} + \sum_{j=1}^{B} \frac{\bar{\pi}_{2j}\lambda_{-1}^{j-1}}{\prod_{h=1}^{j} c_{2h}} + \sum_{j=1}^{B-1} \frac{\bar{\pi}_{2j+3}\lambda_{-1}^{j-1}}{\prod_{h=1}^{j} c_{2h}}. \tag{50}$$

After substituting $\bar{v}_{31}$ from (46) into (42) and then solving (42) and (50), $\bar{v}_{10}$ is given by

$$\bar{v}_{10} = \frac{\bar{\pi}_1}{c_0\lambda_{-1}} + \sum_{j=1}^{B} \frac{\bar{\pi}_{2j}\lambda_{-1}^{j-1}}{\prod_{h=0}^{j} c_{2h}} + \sum_{j=0}^{B-1} \frac{\bar{\pi}_{2j+3}\lambda_{-1}^{j-1}}{\prod_{h=0}^{j} c_{2h}}, \tag{51}$$

where $c_0 = \eta\left(\frac{1}{\lambda_{-1}} - \frac{1}{c_2}\right)$. Note that the set $\{c_0, c_2, \cdots, c_{2B}\}$ contains positive real numbers, and hence we observe from (51) that $\bar{v}_{10} \ge 0$. Thus, from (49) and (50), we deduce that

$\bar{v}_{q0} \geq 0, q \in \mathrm{r}_1$. As a result, we observe from (46) that $\bar{v}_{q0} \geq 0$ and $\bar{v}_{q1} \geq 0, q \in \mathrm{r}_2$. Finally, from (42)-(45), one can easily see that $\bar{v}_{q1} \geq 0, q \in \mathrm{r}_1$, and hence there exists a non-negative limit $\bar{\mathbf{v}}_q, \forall q \in \mathcal{Q}$, satisfying (42)-(46).

Now, we proceed with evaluating the average AoI of source 1. Summing (42)-(45) gives

$$\lambda \sum_{q \in \mathrm{r}_1/\{1\}} \bar{v}_{q0} = \mu \sum_{q \in \mathrm{r}_2} \bar{v}_{q1} + \sum_{q \in \mathrm{r}_1} \bar{\pi}_q. \tag{52}$$

Further, by summing the set of equations in (46), we have

$$\mu \sum_{q \in \mathrm{r}_2} \bar{v}_{q0} = \lambda \sum_{q \in \mathrm{r}_1/\{1\}} \bar{v}_{q0} + \sum_{q \in \mathrm{r}_2} \bar{\pi}_q, \tag{53}$$

$$\mu \sum_{q \in \mathrm{r}_2} \bar{v}_{q1} = \lambda_{-1} \sum_{q \in \mathrm{r}_1/\{1\}} \bar{v}_{q0} + \sum_{q \in \mathrm{r}_2} \bar{\pi}_q. \tag{54}$$

Thus, the average AoI of source 1 can be evaluated as

$$\begin{aligned} \overset{\mathrm{WP}}{\Delta}_{1,1} &= \sum_{q \in \mathrm{r}_1 \cup \mathrm{r}_2} \bar{v}_{q0} \overset{(a)}{=} (1+\rho) \sum_{q \in \mathrm{r}_1/\{1\}} \bar{v}_{q0} + \frac{\sum_{q \in \mathrm{r}_2} \bar{\pi}_q}{\mu} \\ &+ \bar{v}_{10} \overset{(b)}{=} \frac{1+\rho}{\mu\rho_1} + \frac{\sum_{q \in \mathrm{r}_2} \bar{\pi}_q}{\mu} + \bar{v}_{10}, \end{aligned} \tag{55}$$

where step (a) follows from substituting $\sum_{q \in \mathrm{r}_2} \bar{v}_{q0}$ from (53) into (55), and step (b) follows from substituting $\sum_{q \in \mathrm{r}_1} \bar{v}_{q0}$ using (52) and (54) into (55). The final expression of $\overset{\mathrm{WP}}{\Delta}_{1,1}$ in (15) can directly be obtained by substituting $\bar{v}_{10}$ from (51) into (55). ∎

B. Proof of Theorem 2

By inspecting Fig. 3, we observe that the set of equations in (6) corresponding to the states in r_1 are still given by (42)-(45). Regarding the states in r_2, we have

$$\begin{aligned} q_{2k+1}: \ (\lambda+\mu)\,[\bar{v}_{2k+1,0}, \bar{v}_{2k+1,1}] &= [\lambda \bar{v}_{2k,0}, \lambda_{-1} \bar{v}_{2k,0}] \\ + [\lambda \bar{v}_{2k+1,0}, \lambda_{-1} \bar{v}_{2k+1,0}] &+ [\bar{\pi}_{2k+1}, \bar{\pi}_{2k+1}], \end{aligned} \tag{56}$$

where $1 \leq k \leq B$. Similar to the procedure in (47)-(51) in Appendix A, repeated application of (44) gives

$$\begin{aligned} \bar{v}_{2k,0} = \frac{\eta \bar{v}_{2k-2}}{c_{2k}} &+ \sum_{j=1}^{B+1-k} \frac{\bar{\pi}_{2(k+j-1)} \lambda_{-1}^{j-1}}{\prod_{h=1}^{j} c_{2(k+h-1)}} \\ + \frac{1+\rho_{-1}}{1+\rho} &\sum_{j=1}^{B-k} \frac{\bar{\pi}_{2(k+j-1)+3} \lambda_{-1}^{j-1}}{\prod_{h=1}^{j} c_{2(k+h-1)}}, \ 2 \leq k \leq B, \end{aligned} \tag{57}$$

$$\bar{v}_{20} = \frac{\eta \bar{v}_{10}}{c_2} + \sum_{j=1}^{B} \frac{\bar{\pi}_{2j} \lambda_{-1}^{j-1}}{\prod_{h=1}^{j} c_{2h}} + \frac{1+\rho_{-1}}{1+\rho} \sum_{j=1}^{B-1} \frac{\bar{\pi}_{2j+3} \lambda_{-1}^{j-1}}{\prod_{h=1}^{j} c_{2h}}. \tag{58}$$

Thus, from (42), (56) and (58), $\bar{v}_{10}$ can be expressed as

$$\bar{v}_{10} = \frac{\bar{\pi}_1}{c_0 \lambda_{-1}} + \sum_{j=1}^{B} \frac{\bar{\pi}_{2j} \lambda_{-1}^{j-1}}{\prod_{h=0}^{j} c_{2h}} + \frac{1+\rho_{-1}}{1+\rho} \sum_{j=0}^{B-1} \frac{\bar{\pi}_{2j+3} \lambda_{-1}^{j-1}}{\prod_{h=0}^{j} c_{2h}}. \tag{59}$$

Recalling that the set $\{c_0, c_2, \cdots, c_{2B}\}$ contains positive real numbers, we deduce from (42)-(45) and (56)-(59) that there exists a non-negative limit $\bar{\mathbf{v}}_q, \forall q \in \mathcal{Q}$, satisfying (6). Further, the average AoI of source 1 can be evaluated as follows. We first note that $\sum_{q \in \mathrm{r}_1/\{1\}} \bar{v}_{q0}$ and $\sum_{q \in \mathrm{r}_2} \bar{v}_{q0}$ can be expressed as in (52) and (53), respectively. In addition, summing the set of equations in (56) gives

$$(\mu+\lambda) \sum_{q \in \mathrm{r}_2} \bar{v}_{q1} = \lambda_{-1} \sum_{q \in \mathrm{r}_1/\{1\}} \bar{v}_{q0} + \lambda_{-1} \sum_{q \in \mathrm{r}_2} \bar{v}_{q0} + \sum_{q \in \mathrm{r}_2} \bar{\pi}_q. \tag{60}$$

By solving (52), (53) and (60), we get

$$\begin{aligned} \sum_{q \in \mathrm{r}_1/\{1\}} \bar{v}_{q0} &= \frac{1+\rho_{-1}}{\mu\rho_1\,(1+\rho)} + \frac{\sum_{q \in \mathrm{r}_1} \bar{\pi}_q}{\mu\,(1+\rho)}, \\ \sum_{q \in \mathrm{r}_2} \bar{v}_{q0} &= \frac{\rho\,(1+\rho_{-1})}{\mu\rho_1\,(1+\rho)} + \frac{\rho \sum_{q \in \mathrm{r}_1} \bar{\pi}_q}{\mu\,(1+\rho)} + \frac{\sum_{q \in \mathrm{r}_2} \bar{\pi}_q}{\mu}. \end{aligned} \tag{61}$$

From (61), the average AoI of source 1 can be evaluated as

$$\overset{\mathrm{PS}}{\Delta}_{1,1} = \sum_{q \in \mathrm{r}_1 \cup \mathrm{r}_2} \bar{v}_{q0} = \frac{1+\rho}{\mu\rho_1} + \bar{v}_{10}. \tag{62}$$

The expression of $\overset{\mathrm{PS}}{\Delta}_{1,1}$ in (19) can be obtained by substituting $\bar{v}_{10}$ from (59) into (62). ∎

C. Proof of Theorem 4

Using Table II, the set of equations in (8) can be expressed as

$$q_1: \ (\eta - s)\,[\bar{v}^s_{10}, \bar{v}^s_{11}] = \mu[\bar{v}^s_{31}, \bar{\pi}_3], \tag{63}$$

$$q_2: \ (\eta + \lambda - s)\,[\bar{v}^s_{20}, \bar{v}^s_{21}] = \mu[\bar{v}^s_{51}, \bar{\pi}_5] + \eta[\bar{v}^s_{10}, \bar{\pi}_1], \tag{64}$$

$$\begin{aligned} q_{2k}, 2 \leq k \leq B-1: \ (\eta + \lambda - s)\,[\bar{v}^s_{2k,0}, \bar{v}^s_{2k,1}] &= \\ \mu[\bar{v}^s_{2k+3,1}, \bar{\pi}_{2k+3}] + \eta[\bar{v}^s_{2k-2,0}, \bar{\pi}_{2k-2}], \end{aligned} \tag{65}$$

$$q_{2B}: \ (\lambda - s)\,[\bar{v}^s_{2B,0}, \bar{v}^s_{2B,1}] = \eta[\bar{v}^s_{2B-2,0}, \bar{\pi}_{2B-2}], \tag{66}$$

$$\begin{aligned} q_{2k+1}, 1 \leq k \leq B: \ (\mu - s)\,[\bar{v}^s_{2k+1,0}, \bar{v}^s_{2k+1,1}] &= \\ \lambda_1[\bar{v}^s_{2k,0}, \bar{\pi}_{2k}] + \lambda_2[\bar{v}^s_{2k,0}, \bar{v}^s_{2k,0}]. \end{aligned} \tag{67}$$

Summing the set of equations in (63)-(66) gives

$$(\lambda - s) \sum_{q \in \mathrm{r}_1} \bar{v}^s_{q0} = \mu \sum_{q \in \mathrm{r}_2} \bar{v}^s_{q1} + \lambda \bar{v}^s_{10}. \tag{68}$$

Further, by summing the set of equations in (67), we get

$$(\mu - s) \sum_{q \in \mathrm{r}_2} \bar{v}^s_{q0} = \lambda \sum_{q \in \mathrm{r}_1} \bar{v}^s_{q0} - \lambda \bar{v}^s_{10}. \tag{69}$$

$$(\mu - s) \sum_{q \in \mathrm{r}_2} \bar{v}^s_{q1} = \lambda_1 \sum_{q \in \mathrm{r}_1/\{1\}} \bar{\pi}_q + \lambda_2 \sum_{q \in \mathrm{r}_1/\{1\}} \bar{v}^s_{q0}. \tag{70}$$

From (11), the MGF of AoI of source 1 at the destination can be evaluated as

$$\overset{\text{WP}}{M}_1(\bar{s}) = \sum_{q\in \text{r}_1\cup \text{r}_2} \bar{v}^s_{q0} \overset{\text{(a)}}{=} \frac{(\lambda+\mu-s)\sum_{q\in \text{r}_1}\bar{v}^s_{q0} - \lambda\bar{v}^s_{10}}{\mu-s}, \overset{\text{(b)}}{=} \frac{\rho_1(1+\rho-\bar{s})\sum_{q\in \text{r}_1/\{1\}}\bar{\pi}_q + \bar{v}^s_{10}\rho_1(1-\bar{s})}{(1-\bar{s})\left[(1-\bar{s})(\rho-\bar{s})-\rho_{-1}\right]}, \tag{71}$$

where step (a) follows from substituting (69) into (71), and step (b) follows from obtaining $\sum_{q\in \text{r}_1}\bar{v}^s_{q0}$ from (68)-(70) as $\frac{\rho_1\sum_{q\in \text{r}_1/\{1\}}\bar{\pi}_q+\bar{v}^s_{10}(\rho_1-\rho\bar{s})}{(1-\bar{s})(\rho-\bar{s})-\rho_{-1}}$ and substituting it into (71). Finally, $\bar{v}^s_{10}$ in (32) can be obtained by following similar steps as in (47)-(51). ∎

REFERENCES

[1] M. A. Abd-Elmagid and H. S. Dhillon, "Distribution of AoI in EH-powered multi-source systems with source-aware packet management," in *Proc., IEEE Intl. Conf. on Commun. (ICC)*, 2022.

[2] ——, "Distribution of AoI in EH-powered multi-source systems under non-preemptive and preemptive policies," in *Proc., IEEE INFOCOM Workshops*, 2022.

[3] M. A. Abd-Elmagid, N. Pappas, and H. S. Dhillon, "On the role of age of information in the Internet of things," *IEEE Commun. Magazine*, vol. 57, no. 12, pp. 72–77, Dec. 2019.

[4] A. Roy, F. H. Kumbhar, H. S. Dhillon, N. Saxena, S. Y. Shin, and S. Singh, "Efficient monitoring and contact tracing for covid-19: A smart IoT-based framework," *IEEE Internet of Things Magazine*, vol. 3, no. 3, pp. 17–23, Sept. 2020.

[5] S. Kaul, R. Yates, and M. Gruteser, "Real-time status: How often should one update?" in *Proc., IEEE INFOCOM*, 2012.

[6] M. A. Abd-Elmagid, M. A. Kishk, and H. S. Dhillon, "Joint energy and SINR coverage in spatially clustered RF-powered IoT network," *IEEE Trans. on Green Commun. and Networking*, vol. 3, no. 1, pp. 132–146, March 2019.

[7] M. Costa, M. Codreanu, and A. Ephremides, "On the age of information in status update systems with packet management," *IEEE Trans. on Info. Theory*, vol. 62, no. 4, pp. 1897–1910, Apr. 2016.

[8] S. K. Kaul, R. D. Yates, and M. Gruteser, "Status updates through queues," in *Proc., IEEE Conf. on Info. Sciences and Systems (CISS)*, 2012.

[9] A. Soysal and S. Ulukus, "Age of information in G/G/1/1 systems: Age expressions, bounds, special cases, and optimization," *IEEE Trans. on Info. Theory*, to appear.

[10] K. Chen and L. Huang, "Age-of-information in the presence of error," in *Proc., IEEE Intl. Symposium on Information Theory*, 2016.

[11] C. Kam, S. Kompella, G. D. Nguyen, J. E. Wieselthier, and A. Ephremides, "On the age of information with packet deadlines," *IEEE Trans. on Info. Theory*, vol. 64, no. 9, pp. 6419–6428, Sept. 2018.

[12] V. Kavitha, E. Altman, and I. Saha, "Controlling packet drops to improve freshness of information," 2018, available online: arxiv.org/abs/1807.09325.

[13] P. Zou, O. Ozel, and S. Subramaniam, "Waiting before serving: A companion to packet management in status update systems," *IEEE Trans. on Info. Theory*, vol. 66, no. 6, pp. 3864–3877, June 2019.

[14] Y. Inoue, H. Masuyama, T. Takine, and T. Tanaka, "A general formula for the stationary distribution of the age of information and its application to single-server queues," *IEEE Trans. Info. Theory*, vol. 65, no. 12, pp. 8305–8324, Dec. 2019.

[15] A. Kosta, N. Pappas, A. Ephremides, and V. Angelakis, "The age of information in a discrete time queue: Stationary distribution and non-linear age mean analysis," *IEEE Journal on Sel. Areas in Commun.*, vol. 39, no. 5, pp. 1352–1364, May 2021.

[16] J. P. Champati, H. Al-Zubaidy, and J. Gross, "On the distribution of AoI for the GI/GI/1/1 and GI/GI/1/2* systems: Exact expressions and bounds," in *Proc., IEEE INFOCOM*, 2019.

[17] F. Chiariotti, O. Vikhrova, B. Soret, and P. Popovski, "Peak age of information distribution for edge computing with wireless links," *IEEE Trans. on Commun.*, vol. 69, no. 5, pp. 3176–3191, May 2021.

[18] O. Ayan, H. M. Gürsu, A. Papa, and W. Kellerer, "Probability analysis of age of information in multi-hop networks," *IEEE Networking Letters*, vol. 2, no. 2, pp. 76–80, June 2020.

[19] O. Vikhrova, F. Chiariotti, B. Soret, G. Araniti, A. Molinaro, and P. Popovski, "Age of information in multi-hop networks with priorities," in *Proc., IEEE Globecom*, 2020.

[20] R. D. Yates and S. Kaul, "Real-time status updating: Multiple sources," in *Proc., IEEE Intl. Symposium on Information Theory*, 2012.

[21] M. Moltafet, M. Leinonen, and M. Codreanu, "On the age of information in multi-source queueing models," *IEEE Trans. on Commun.*, vol. 68, no. 8, pp. 5003–5017, Aug. 2020.

[22] N. Pappas, J. Gunnarsson, L. Kratz, M. Kountouris, and V. Angelakis, "Age of information of multiple sources with queue management," in *Proc., IEEE Intl. Conf. on Commun. (ICC)*, 2015.

[23] R. D. Yates and S. K. Kaul, "Status updates over unreliable multiaccess channels," in *Proc., IEEE Intl. Symposium on Information Theory*, 2017.

[24] A. Kosta, N. Pappas, A. Ephremides, and V. Angelakis, "Age of information performance of multiaccess strategies with packet management," *Journal of Commun. and Networks*, vol. 21, no. 3, pp. 244–255, June 2019.

[25] E. Najm and E. Telatar, "Status updates in a multi-stream m/g/1/1 preemptive queue," in *Proc., IEEE INFOCOM Workshops*, 2018.

[26] L. Huang and E. Modiano, "Optimizing age-of-information in a multi-class queueing system," in *Proc., IEEE Intl. Symposium on Information Theory*, 2015.

[27] J. Xu and N. Gautam, "Peak age of information in priority queuing systems," *IEEE Trans. on Info. Theory*, vol. 67, no. 1, pp. 373–390, Jan. 2021.

[28] N. Akar, "Discrete-time queueing model of age of information with multiple information sources," *IEEE Internet of Things Journal*, to appear.

[29] O. Dogan and N. Akar, "The multi-source probabilistically preemptive m/ph/1/1 queue with packet errors," *IEEE Trans. on Commun.*, to appear.

[30] R. D. Yates and S. K. Kaul, "The age of information: Real-time status updating by multiple sources," *IEEE Trans. on Info. Theory*, vol. 65, no. 3, pp. 1807–1827, Mar. 2019.

[31] R. D. Yates, "The age of information in networks: Moments, distributions, and sampling," *IEEE Trans. on Info. Theory*, vol. 66, no. 9, pp. 5712–5728, Sept. 2020.

[32] J. P. Hespanha, "Modelling and analysis of stochastic hybrid systems," *IEE Proceedings-Control Theory and Applications*, vol. 153, no. 5, pp. 520–535, Sept. 2006.

[33] A. Maatouk, M. Assaad, and A. Ephremides, "On the age of information in a csma environment," *IEEE/ACM Trans. on Networking*, vol. 28, no. 2, pp. 818–831, Apr. 2020.

[34] M. Moltafet, M. Leinonen, and M. Codreanu, "Average AoI in multi-source systems with source-aware packet management," *IEEE Trans. on Commun.*, vol. 69, no. 2, pp. 1121–1133, Feb. 2021.

[35] A. Javani, M. Zorgui, and Z. Wang, "Age of information for multiple-source multiple-server networks," 2021, available online: arxiv.org/abs/2106.07247.

[36] M. Moltafet, M. Leinonen, and M. Codreanu, "Moment generating function of the AoI in a two-source system with packet management," *IEEE Wireless Commun. Letters*, vol. 10, no. 4, pp. 882–886, Apr. 2021.

[37] R. D. Yates, "Lazy is timely: Status updates by an energy harvesting source," in *Proc., IEEE Intl. Symposium on Information Theory*, 2015.

[38] X. Zheng, S. Zhou, Z. Jiang, and Z. Niu, "Closed-form analysis of non-linear age of information in status updates with an energy harvesting transmitter," *IEEE Trans. on Wireless Commun.*, vol. 18, no. 8, pp. 4129–4142, Aug. 2019.

[39] S. Farazi, A. G. Klein, and D. R. Brown, "Average age of information for status update systems with an energy harvesting server," in *Proc., IEEE INFOCOM Workshops*, 2018.

[40] S. Farazi, A. G. Klein, and D. R. Brown, "Age of information in energy harvesting status update systems: When to preempt in service?" in *Proc., IEEE Intl. Symposium on Information Theory*, 2018.

[41] M. A. Abd-Elmagid and H. S. Dhillon, "Closed-form characterization of the MGF of AoI in energy harvesting status update systems," *IEEE Trans. on Info. Theory*, to appear.

[42] R. D. Yates, Y. Sun, D. R. Brown, S. K. Kaul, E. Modiano, and S. Ulukus, "Age of information: An introduction and survey," *EEE Journal on Selected Areas in Commun.*, vol. 39, no. 5, pp. 1183–1210, May 2021.

[43] B. T. Bacinoglu, E. T. Ceran, and E. Uysal-Biyikoglu, "Age of information under energy replenishment constraints," in *Proc., Information Theory and its Applications (ITA)*, 2015.

[44] X. Wu, J. Yang, and J. Wu, "Optimal status update for age of information minimization with an energy harvesting source," *IEEE Trans. on Green Commun. and Networking*, vol. 2, no. 1, pp. 193–204, Mar. 2018.

[45] S. Leng and A. Yener, "Age of information minimization for an energy harvesting cognitive radio," *IEEE Trans. on Cognitive Commun. and Networking*, vol. 5, no. 2, pp. 427–439, June 2019.

[46] A. Arafa, J. Yang, S. Ulukus, and H. V. Poor, "Age-minimal transmission for energy harvesting sensors with finite batteries: Online policies," *IEEE Trans. on Info. Theory*, vol. 66, no. 1, pp. 534–556, Jan. 2020.

[47] M. A. Abd-Elmagid, H. S. Dhillon, and N. Pappas, "Online age-minimal sampling policy for RF-powered IoT networks," in *Proc., IEEE Globecom*, 2019.

[48] M. Hatami, M. Jahandideh, M. Leinonen, and M. Codreanu, "Age-aware status update control for energy harvesting iot sensors via reinforcement learning," in *Proc., IEEE PIMRC*, 2020.

[49] M. A. Abd-Elmagid, H. S. Dhillon, and N. Pappas, "A reinforcement learning framework for optimizing age of information in RF-powered communication systems," *IEEE Trans. on Commun.*, vol. 68, no. 8, pp. 4747 – 4760, Aug. 2020.

[50] M. A. Abd-Elmagid, H. S. Dhillon, and N. Pappas, "AoI-optimal joint sampling and updating for wireless powered communication systems," *IEEE Trans. on Veh. Technology*, vol. 69, no. 11, pp. 14 110–14 115, Nov. 2020.

[51] E. Gindullina, L. Badia, and D. Gündüz, "Age-of-information with information source diversity in an energy harvesting system," *IEEE Trans. on Green Commun. and Networking*, vol. 5, no. 3, pp. 1529–1540, Sept. 2021.

[52] Y. Khorsandmanesh, M. J. Emadi, and I. Krikidis, "Average peak age of information analysis for wireless powered cooperative networks," *IEEE Trans. on Cognitive Commun. and Networking*, to appear.

[53] A. Arafa, J. Yang, S. Ulukus, and H. V. Poor, "Timely status updating over erasure channels using an energy harvesting sensor: Single and multiple sources," *IEEE Trans. on Green Commun. and Networking*, to appear.

[54] N. Nouri, D. Ardan, and M. M. Feghhi, "Age of information-reliability trade-offs in energy harvesting sensor networks," 2020, available online: arxiv.org/abs/2008.00987.

[55] Y. Sun, E. Uysal-Biyikoglu, R. D. Yates, C. E. Koksal, and N. B. Shroff, "Update or wait: How to keep your data fresh," *IEEE Trans. on Info. Theory*, vol. 63, no. 11, pp. 7492–7508, Nov. 2017.

[56] Q. He, D. Yuan, and A. Ephremides, "Optimal link scheduling for age minimization in wireless systems," *IEEE Trans. on Info. Theory*, vol. 64, no. 7, pp. 5381–5394, July 2018.

[57] B. Han, Y. Zhu, Z. Jiang, M. Sun, and H. D. Schotten, "Fairness for freshness: Optimal age of information based OFDMA scheduling with minimal knowledge," *IEEE Trans. on Wiress Commun.*, to appear.

[58] T. Z. Ornee and Y. Sun, "Sampling for remote estimation through queues: Age of information and beyond," in *Proc., Modeling and Optimization in Mobile, Ad Hoc and Wireless Networks*, 2019.

[59] M. K. Abdel-Aziz, C.-F. Liu, S. Samarakoon, M. Bennis, and W. Saad, "Ultra-reliable low-latency vehicular networks: Taming the age of information tail," in *Proc., IEEE Globecom*, 2018.

[60] M. A. Abd-Elmagid and H. S. Dhillon, "Average peak age-of-information minimization in UAV-assisted IoT networks," *IEEE Trans. on Veh. Technology*, vol. 68, no. 2, pp. 2003–2008, Feb. 2019.

[61] M. A. Abd-Elmagid, A. Ferdowsi, H. S. Dhillon, and W. Saad, "Deep reinforcement learning for minimizing age-of-information in UAV-assisted networks," in *Proc., IEEE Globecom*, 2019.

[62] A. Ferdowsi, M. A. Abd-Elmagid, W. Saad, and H. S. Dhillon, "Neural combinatorial deep reinforcement learning for age-optimal joint trajectory and scheduling design in uav-assisted networks," *IEEE Journal on Selected Areas in Commun.*, vol. 39, no. 5, pp. 1250–1265, May 2021.

[63] M. Emara, H. Elsawy, and G. Bauch, "A spatiotemporal model for peak AoI in uplink IoT networks: Time versus event-triggered traffic," *IEEE Internet Things Journal*, vol. 7, no. 8, pp. 6762–6777, Aug. 2020.

[64] P. D. Mankar, M. A. Abd-Elmagid, and H. S. Dhillon, "Spatial distribution of the mean peak age of information in wireless networks," *IEEE Trans. on Wireless Commun.*, vol. 20, no. 7, pp. 4465–4479, July 2021.

[65] P. D. Mankar, Z. Chen, M. A. Abd-Elmagid, N. Pappas, and H. S. Dhillon, "Throughput and age of information in a cellular-based IoT network," *IEEE Trans. on Wireless Commun., to appear*.

[66] H. Tang, P. Ciblat, J. Wang, M. Wigger, and R. Yates, "Age of information aware cache updating with file-and age-dependent update durations," in *Proc., Modeling and Optimization in Mobile, Ad Hoc and Wireless Networks*, 2020.

[67] M. Ma and V. W. Wong, "Age of information driven cache content update scheduling for dynamic contents in heterogeneous networks," *IEEE Trans. on Wireless Commun.*, vol. 19, no. 12, pp. 8427–8441, Dec. 2020.

[68] M. Bastopcu and S. Ulukus, "Information freshness in cache updating systems," *IEEE Trans. on Wireless Commun.*, vol. 20, no. 3, pp. 1861–1874, Mar. 2021.

[69] H. H. Yang, A. Arafa, T. Q. Quek, and H. V. Poor, "Age-based scheduling policy for federated learning in mobile edge networks," in *Proc., IEEE Intl. Conf. on Acoustics, Speech, and Sig. Proc. (ICASSP)*, 2020.

[70] B. Buyukates and S. Ulukus, "Timely communication in federated learning," in *Proc., IEEE INFOCOM Workshops*, 2021.

[71] R. Jain, D.-M. Chiu, and W. Hawe, "A quantitative measure of fairness and discrimination for resource allocation in shared computer systems," *DEC Research Repor, Technical Report TR-301*, Sept. 1984.

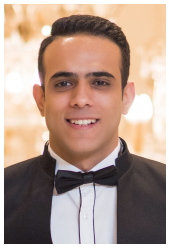

Mohamed A. Abd-Elmagid (Member, IEEE) received the B.Sc. degree in electronics and electrical communications engineering from Cairo University, Egypt, in 2014, and the M.S. degree in wireless communications from Nile University, Egypt, in 2017. He is currently pursuing the Ph.D. degree with the Bradley Department of Electrical and Computer Engineering, Virginia Tech. His research interests include age of information, energy harvesting, optimization, machine learning, queueing theory, and stochastic geometry. He has received the WiOpt 2021 best student paper award.

Harpreet S. Dhillon (S'11–M'13–SM'19) received the B.Tech. degree in electronics and communication engineering from IIT Guwahati in 2008, the M.S. degree in electrical engineering from Virginia Tech in 2010, and the Ph.D. degree in electrical engineering from the University of Texas at Austin in 2013. After serving as a Viterbi Postdoctoral Fellow at the University of Southern California for a year, he joined Virginia Tech in 2014, where he is currently an Associate Professor of electrical and computer engineering and the Elizabeth and James E. Turner Jr. '56 Faculty Fellow. His research interests include communication theory, wireless networks, and stochastic geometry. He is a Clarivate Analytics Highly Cited Researcher and has received six best paper awards including the 2014 IEEE Leonard G. Abraham Prize, the 2015 IEEE ComSoc Young Author Best Paper Award, and the 2016 IEEE Heinrich Hertz Award. He has also received Early Achievement Awards from three IEEE ComSoc Technical Committees, namely, the Communication Theory Technical Committee in 2020, the Radio Communications Committee in 2020, and the Wireless Communications Technical Committee in 2021. He was named the 2017 Outstanding New Assistant Professor, the 2018 Steven O. Lane Junior Faculty Fellow, the 2018 College of Engineering Faculty Fellow, and the recipient of the 2020 Dean's Award for Excellence in Research by Virginia Tech. His other academic honors include the 2008 Agilent Engineering and Technology Award, the UT Austin MCD Fellowship, the 2013 UT Austin WNCG leadership award, and the inaugural IIT Guwahati Young Alumni Achiever Award 2020. He is currently serving as the TPC co-chair for IEEE WCNC 2022 and an Editor for three IEEE journals.

Supplementary Material

D. Proof of Theorem 3

Table IV presents the set of transitions $\mathcal{L}$ and their impact on the values of both $q(t)$ and $\mathbf{x}(t)$. While the description of most transitions in Table IV is similar to the description of their counterparts in Tables II and III, there are some key differences. The first difference is that the second component of the updated age vector $\mathbf{x}\mathbf{A}_l$ in Table IV is set to 0 (rather than x_0 as in Tables II and III) when a new update packet is generated from source $i \in \{2, 3, \cdots, N\}$ at the time when the system is empty (i.e., transition $l = (3N+1)k - 3N + i$) or another packet generated from source i is being served (i.e., transition $l = (3N+1)k - 2N + i$). This is because under the LCFS-SA queueing discipline, we know the index of the source that generated the packet in service, and hence we can safely set the irrelevant second component of $\mathbf{x}\mathbf{A}_l$ to 0 when such transitions l occur. The second difference, which has a similar interpretation to the first one, is that the first component of the updated age vector $\mathbf{x}\mathbf{A}_l$ in Table IV is set to x_0 (rather than x_1 as in Table II) when an update packet generated from source $i \in \{2, 3, \cdots, N\}$ is delivered to the destination (i.e., transition $l = (3N+1)k - N + i$).

Since the second component of the vector $\bar{\mathbf{v}}_{q_l}\mathbf{A}_l (\forall l \in \mathcal{L}'_q$ and $q \in \mathcal{Q})$ is 0, we observe from (6) that $\bar{v}_{q1} \geq 0, \forall q \in \mathcal{Q}$. The existence of a non-negative limit $\bar{\mathbf{v}}_q, \forall q \in \mathcal{Q}$, satisfying (6) is then tied with having $\bar{v}_{q0} \geq 0, \forall q \in \mathcal{Q}$. The set of equations in (6) corresponding to the states in r_1 can be expressed as

$$q_1: \quad \eta \bar{v}_{10} = \mu \bar{v}_{31} + \mu \sum_{j=4}^{N+2} \bar{v}_{j0} + \bar{\pi}_1, \tag{72}$$

$$q_2: \quad (\eta + \lambda)\, \bar{v}_{20} = \eta \bar{v}_{10} + \mu \bar{v}_{N+4,1} + \mu \sum_{j=N+5}^{2N+3} \bar{v}_{j0} + \bar{\pi}_2, \tag{73}$$

$$q_{2+k(N+1)}, 1 \leq k \leq B-2: \quad (\eta + \lambda)\, \bar{v}_{2+k(N+1),0} = \eta \bar{v}_{2+(k-1)(N+1),0} + \mu \bar{v}_{3+(k+1)(N+1),1} + \mu \sum_{j=4+(k+1)(N+1)}^{N+2+(k+1)(N+1)} \bar{v}_{j0} + \bar{\pi}_{2+k(N+1)}, \tag{74}$$

$$q_{2+(B-1)(N+1)}: \quad \lambda \bar{v}_{2+(B-1)(N+1),0} = \eta \bar{v}_{2+(B-2)(N+1),0} + \bar{\pi}_{2+(B-1)(N+1)}. \tag{75}$$

Further, the set of equations in (6) corresponding to the states in r_{i+1}, $1 \leq i \leq N$, can be expressed as

$$q_{2+i+k(N+1)}, 0 \leq k \leq B-1: \quad \mu \bar{v}_{2+i+k(N+1),0} = \lambda_i \bar{v}_{2+k(N+1),0} + \bar{\pi}_{2+i+k(N+1)}. \tag{76}$$

By noting that $\bar{v}_{3+k(N+1),1} = \dfrac{\bar{\pi}_{3+k(N+1)}}{\mu + \lambda_1}, 0 \leq k \leq B-1$, (74) can be rewritten as

$$q_{2+k(N+1)}: \quad (\eta + \lambda)\, \bar{v}_{2+k(N+1),0} = \eta \bar{v}_{2+(k-1)(N+1),0} + \lambda_{-1} \bar{v}_{2+(k+1)(N+1),0} + \bar{\pi}_{2+k(N+1)} + \frac{\mu \bar{\pi}_{3+(k+1)(N+1)}}{\mu + \lambda_1} + \sum_{j=4+(k+1)(N+1)}^{N+2+(k+1)(N+1)} \bar{\pi}_j, \tag{77}$$

where $1 \leq k \leq B-2$, and $\sum_{j=4+(k+1)(N+1)}^{N+2+(k+1)(N+1)} \bar{v}_{j0}$ in (74) was substituted from (76). Now, repeated application of (77) gives

$$\bar{v}_{2+k(N+1),0} = \frac{\eta \bar{v}_{2+(k-1)(N+1),0}}{\bar{c}_k} + \sum_{j=1}^{B-k} \frac{\bar{\pi}_{2+(k+j-1)(N+1)} \left(\mu \rho_{-1}\right)^{j-1}}{\prod_{h=1}^{j} \bar{c}_{k+h-1}} + \sum_{j=1}^{B-k-1} \frac{\frac{\bar{\pi}_{3+(k+j)(N+1)}}{1+\rho_1} + \sum_{m=4+(k+j)(N+1)}^{1+(k+j+1)(N+1)} \bar{\pi}_m}{\prod_{h=1}^{j} \bar{c}_{k+h-1}} \left(\mu \rho_{-1}\right)^{j-1}, \; 1 \leq k \leq B-1, \tag{78}$$

$$\bar{v}_{2,0} = \frac{\eta \bar{v}_{1,0}}{\bar{c}_0} + \sum_{j=1}^{B} \frac{\bar{\pi}_{2+(j-1)(N+1)} \left(\mu \rho_{-1}\right)^{j-1}}{\prod_{h=1}^{j} \bar{c}_{h-1}} + \sum_{j=1}^{B-1} \frac{\frac{\bar{\pi}_{3+j(N+1)}}{1+\rho_1} + \sum_{m=4+j(N+1)}^{1+(j+1)(N+1)} \bar{\pi}_m}{\prod_{h=1}^{j} \bar{c}_{h-1}} \left(\mu \rho_{-1}\right)^{j-1}, \tag{79}$$

where the set $\{\bar{c}_h\}$ is defined in (27). The expression of $\bar{v}_{10}$ in (26) can be obtained by solving (72) and (79) while noting that $\bar{v}_{31} = \frac{\bar{\pi}_3}{\mu + \lambda_1}$ and $\mu \sum_{j=4}^{N+2} \bar{v}_{j0} = \lambda_{-1} \bar{v}_{20} + \sum_{j=4}^{N+2} \bar{\pi}_j$. Since the set $\{\bar{c}_{-1}, \bar{c}_0, \cdots, \bar{c}_{B-1}\}$ contains positive real numbers, we have $\bar{v}_{10} \geq 0$. Therefore, from (76), (78) and (79), we observe that $\bar{v}_{q0} \geq 0, \forall q \in \mathcal{Q}$, and hence there exits a non-negative

TABLE IV
TRANSITIONS OF THE LCFS-SA QUEUEING DISCIPLINE IN FIG. 4 ($2 \leq i \leq N,\ 2 \leq k \leq B$).

l	$q_l \to q_l'$	$\lambda^{(l)}$	$\mathbf{x}\mathbf{A}_l$	$\mathbf{A}_l$	$\hat{\mathbf{A}}_l$	$\bar{\mathbf{v}}_{q_l}\mathbf{A}_l$	$\bar{\pi}_{q_l}\mathbf{1}\hat{\mathbf{A}}_l$
1	$1 \to 2$	η	$[x_0, 0]$	$\begin{bmatrix} 1 & 0 \\ 0 & 0 \end{bmatrix}$	$\begin{bmatrix} 0 & 0 \\ 0 & 1 \end{bmatrix}$	$[\bar{v}_{10}, 0]$	$[0, \bar{\pi}_1]$
2	$2 \to 3$	λ_1	$[x_0, 0]$	$\begin{bmatrix} 1 & 0 \\ 0 & 0 \end{bmatrix}$	$\begin{bmatrix} 0 & 0 \\ 0 & 1 \end{bmatrix}$	$[\bar{v}_{20}, 0]$	$[0, \bar{\pi}_2]$
$1+i$	$2 \to 2+i$	λ_i	$[x_0, 0]$	$\begin{bmatrix} 1 & 0 \\ 0 & 0 \end{bmatrix}$	$\begin{bmatrix} 0 & 0 \\ 0 & 1 \end{bmatrix}$	$[\bar{v}_{20}, 0]$	$[0, \bar{\pi}_2]$
$2+N$	$3 \to 3$	λ_1	$[x_0, 0]$	$\begin{bmatrix} 1 & 0 \\ 0 & 0 \end{bmatrix}$	$\begin{bmatrix} 0 & 0 \\ 0 & 1 \end{bmatrix}$	$[\bar{v}_{30}, 0]$	$[0, \bar{\pi}_3]$
$1+N+i$	$2+i \to 2+i$	λ_i	$[x_0, 0]$	$\begin{bmatrix} 1 & 0 \\ 0 & 0 \end{bmatrix}$	$\begin{bmatrix} 0 & 0 \\ 0 & 1 \end{bmatrix}$	$[\bar{v}_{2+i,0}, 0]$	$[0, \bar{\pi}_{2+i}]$
$2\,(N+1)$	$3 \to 1$	μ	$[x_1, 0]$	$\begin{bmatrix} 0 & 0 \\ 1 & 0 \end{bmatrix}$	$\begin{bmatrix} 0 & 0 \\ 0 & 1 \end{bmatrix}$	$[\bar{v}_{31}, 0]$	$[0, \bar{\pi}_3]$
$1+2N+i$	$2+i \to 1$	μ	$[x_0, 0]$	$\begin{bmatrix} 1 & 0 \\ 0 & 0 \end{bmatrix}$	$\begin{bmatrix} 0 & 0 \\ 0 & 1 \end{bmatrix}$	$[\bar{v}_{2+i,0}, 0]$	$[0, \bar{\pi}_{2+i}]$
$(3N+1)\,k-3N$	$2+(N+1)(k-2) \to 2+(N+1)(k-1)$	η	$[x_0, 0]$	$\begin{bmatrix} 1 & 0 \\ 0 & 0 \end{bmatrix}$	$\begin{bmatrix} 0 & 0 \\ 0 & 1 \end{bmatrix}$	$[\bar{v}_{2+(N+1)(k-2),0}, 0]$	$[0, \bar{\pi}_{2+(N+1)(k-2)}]$
$(3N+1)\,k-3N+1$	$2+(N+1)(k-2) \to 3+(N+1)(k-2)$	λ_1	$[x_0, 0]$	$\begin{bmatrix} 1 & 0 \\ 0 & 0 \end{bmatrix}$	$\begin{bmatrix} 0 & 0 \\ 0 & 1 \end{bmatrix}$	$[\bar{v}_{2+(N+1)(k-2),0}, 0]$	$[0, \bar{\pi}_{2+(N+1)(k-2)}]$
$(3N+1)\,k-3N+i$	$2+(N+1)(k-2) \to 2+i+(N+1)(k-2)$	λ_i	$[x_0, 0]$	$\begin{bmatrix} 1 & 0 \\ 0 & 0 \end{bmatrix}$	$\begin{bmatrix} 0 & 0 \\ 0 & 1 \end{bmatrix}$	$[\bar{v}_{2+(N+1)(k-2),0}, 0]$	$[0, \bar{\pi}_{2+(N+1)(k-2)}]$
$(3N+1)\,k-2N+1$	$3+(N+1)(k-2) \to 3+(N+1)(k-2)$	λ_1	$[x_0, 0]$	$\begin{bmatrix} 1 & 0 \\ 0 & 0 \end{bmatrix}$	$\begin{bmatrix} 0 & 0 \\ 0 & 1 \end{bmatrix}$	$[\bar{v}_{3+(N+1)(k-2),0}, 0]$	$[0, \bar{\pi}_{3+(N+1)(k-2)}]$
$(3N+1)\,k-2N+i$	$2+i+(N+1)(k-2) \to 2+i+(N+1)(k-2)$	λ_i	$[x_0, 0]$	$\begin{bmatrix} 1 & 0 \\ 0 & 0 \end{bmatrix}$	$\begin{bmatrix} 0 & 0 \\ 0 & 1 \end{bmatrix}$	$[\bar{v}_{2+i+(N+1)(k-2),0}, 0]$	$[0, \bar{\pi}_{2+i+(N+1)(k-2)}]$
$(3N+1)k-N+1$	$3+(N+1)(k-1) \to 2+(N+1)(k-2)$	μ	$[x_1, 0]$	$\begin{bmatrix} 0 & 0 \\ 1 & 0 \end{bmatrix}$	$\begin{bmatrix} 0 & 0 \\ 0 & 1 \end{bmatrix}$	$[\bar{v}_{3+(N+1)(k-1),1}, 0]$	$[0, \bar{\pi}_{3+(N+1)(k-1)}]$
$(3N+1)k-N+i$	$2+i+(N+1)(k-1) \to 2+(N+1)(k-2)$	μ	$[x_0, 0]$	$\begin{bmatrix} 1 & 0 \\ 0 & 0 \end{bmatrix}$	$\begin{bmatrix} 0 & 0 \\ 0 & 1 \end{bmatrix}$	$[\bar{v}_{2+i+(N+1)(k-1),0}, 0]$	$[0, \bar{\pi}_{2+i+(N+1)(k-1)}]$

limit $\bar{\mathbf{v}}_q, \forall q \in \mathcal{Q}$, satisfying (6). In the following, we evaluate the average AoI of source 1. By summing the equations in (76), we have

$$\mu \sum_{q \in \mathrm{r}_{i+1}} \bar{v}_{q0} = \lambda_i \sum_{q \in \mathrm{r}_1/\{1\}} \bar{v}_{q0} + \sum_{q \in \mathrm{r}_{i+1}} \bar{\pi}_q, \tag{80}$$

where $1 \leq i \leq N$. Further, summing the equations in (72)-(75) gives

$$\lambda \sum_{q \in \mathrm{r}_1/\{1\}} \bar{v}_{q0} = \mu \sum_{q \in \mathrm{r}_2} \bar{v}_{q1} + \mu \sum_{q \in \mathcal{Q}/(\mathrm{r}_1 \cup \mathrm{r}_2)} \bar{v}_{q0} + \sum_{q \in \mathrm{r}_1} \bar{\pi}_q, \tag{81}$$

where $\sum_{q \in \mathrm{r}_2} \bar{v}_{q1} = \dfrac{\sum_{q \in \mathrm{r}_2} \bar{\pi}_q}{\mu + \lambda_1}$. From (80) and (81), we get

$$\lambda_1 \sum_{q \in \mathrm{r}_1/\{1\}} \bar{v}_{q0} = \frac{\sum_{q \in \mathrm{r}_2} \bar{\pi}_q}{1+\rho_1} + \sum_{q \in \mathcal{Q}/\mathrm{r}_2} \bar{\pi}_q. \tag{82}$$

Hence, the average AoI of source 1 can be obtained as

$$\overset{\text{SA}}{\Delta}_{1,1} = \sum_{q \in \mathcal{Q}} \bar{v}_{q0} \overset{\text{(a)}}{=} \frac{1+\rho}{\mu\rho_1\,(1+\rho_1)} + \frac{(1+\rho)\sum_{q \in \mathcal{Q}/\mathrm{r}_2} \bar{\pi}_q}{\mu\,(1+\rho_1)} + \frac{\sum_{q \in \mathcal{Q}/\mathrm{r}_1} \bar{\pi}_q}{\mu} + \bar{v}_{10}, \tag{83}$$

where step (a) follows from (80) and (82). This completes the proof. ■

E. Proof of Theorem 5

Similar to Appendix B, we first note that the set of equations in (8) corresponding to the states in r_1 are given by (63)-(66), and hence $\sum_{q \in \mathrm{r}_1} \bar{v}^s_{q0}$ can be expressed as in (68). Regarding the states in r_2, we have

$$\begin{aligned} q_{2k+1}, 1 \leq k \leq B: \ & (\mu - s)\,\bar{v}^s_{2k+1,0} = \lambda \bar{v}^s_{2k,0}, \\ & (\lambda + \mu - s)\,\bar{v}^s_{2k+1,1} = \lambda_2(\bar{v}^s_{2k,0} + \bar{v}^s_{2k+1,0}) + \lambda_1(\bar{\pi}_{2k} + \bar{\pi}_{2k+1}). \end{aligned} \tag{84}$$

We observe from (84) that $\sum_{q \in \mathrm{r}_2} \bar{v}^s_{q0}$ is given by (69) and $\sum_{q \in \mathrm{r}_2} \bar{v}^s_{q1}$ can be expressed as

$$(\lambda + \mu - s) \sum_{q \in \mathrm{r}_2} \bar{v}^s_{q1} = \lambda_2 \sum_{q \in \mathcal{Q}/\{1\}} \bar{v}^s_{q0} + \lambda_1\,(1 - \bar{\pi}_1)\,. \tag{85}$$

Hence, the MGF of AoI of source 1 at the destination can be evaluated as

$$\overset{\text{PS}}{M}_1(\bar{s}) = \sum_{q\in\, \mathrm{r}_1\cup\, \mathrm{r}_2} \bar{v}^s_{q0} \overset{\text{(a)}}{=} \frac{(\lambda+\mu-s)\sum_{q\in\, \mathrm{r}_1}\bar{v}^s_{q0} - \lambda\bar{v}^s_{10}}{\mu-s} \overset{\text{(b)}}{=} \frac{\rho_1\left(1-\bar{\pi}_1+\bar{v}^s_{10}\right)}{\left(1-\bar{s}\right)\left(\rho-\bar{s}\right)-\rho_{-1}}, \tag{86}$$

where step (a) follows from substituting (69) into (86), and step (b) follows from obtaining $\sum_{q\in\, \mathrm{r}_1}\bar{v}^s_{q0}$ from (68), (69) and (85) as $\frac{\rho_1(1-\bar{\pi}_1)(1-\bar{s})+\bar{v}^s_{10}(\rho_1-\rho\bar{s})(1+\rho-\bar{s})}{(1+\rho-\bar{s})[(1-\bar{s})(\rho-\bar{s})-\rho_{-1}]}$ and substituting it into (86). Finally, $\bar{v}^s_{10}$ in (37) can be obtained by following similar steps as in (57)-(59). ■

F. Proof of Theorem 6

Using Table IV, the set of equations in (8) corresponding to $q\in \mathrm{r}_1$ can be expressed as

$$q_1:\ \ \left(\eta-s\right)\bar{v}^s_{10} = \mu\bar{v}^s_{31} + \mu\sum_{j=4}^{N+2}\bar{v}^s_{j0}, \tag{87}$$

$$q_2:\ \ \left(\eta+\lambda-s\right)\bar{v}^s_{20} = \eta\bar{v}^s_{10} + \mu\bar{v}^s_{N+4,1} + \mu\sum_{j=N+5}^{2N+3}\bar{v}^s_{j0}, \tag{88}$$

$$q_{2+k(N+1)}, 1\le k\le B-2:\ \ \left(\eta+\lambda-s\right)\bar{v}^s_{2+k(N+1),0} = \eta\bar{v}^s_{2+(k-1)(N+1),0} + \mu\bar{v}^s_{3+(k+1)(N+1),1} + \mu\sum_{j=4+(k+1)(N+1)}^{N+2+(k+1)(N+1)}\bar{v}^s_{j0}, \tag{89}$$

$$q_{2+(B-1)(N+1)}:\ \ \left(\lambda-s\right)\bar{v}^s_{2+(B-1)(N+1),0} = \eta\bar{v}^s_{2+(B-2)(N+1),0}. \tag{90}$$

Further, the set of equations in (8) corresponding to $q\in \mathrm{r}_{i+1}$, $1\le i\le N$, can be expressed as

$$q_{2+i+k(N+1)}, 0\le k\le B-1:\ \ \left(\mu-s\right)\bar{v}^s_{2+i+k(N+1),0} = \lambda_i\bar{v}^s_{2+k(N+1),0}. \tag{91}$$

Summing the equations in (87)-(90) gives

$$\left(\lambda-s\right)\sum_{q\in\, \mathrm{r}_1}\bar{v}^s_{q0} = \mu\sum_{q\in\, \mathrm{r}_2}\bar{v}^s_{q1} + \mu\sum_{q\in\, \mathcal{Q}/(\mathrm{r}_1\cup\, \mathrm{r}_2)}\bar{v}^s_{q0} + \lambda\bar{v}^s_{10}, \tag{92}$$

where $\sum_{q\in\, \mathrm{r}_2}\bar{v}^s_{q1} = \dfrac{\lambda_1\sum_{q\in\, \mathrm{r}_1\cup\, \mathrm{r}_2/\{1\}}\bar{\pi}_q}{(\mu+\lambda_1-s)}$. In addition, by summing the equations in (91), we get

$$\left(\mu-s\right)\sum_{q\in\, \mathrm{r}_{i+1}}\bar{v}^s_{q0} = \lambda_i\sum_{q\in\, \mathrm{r}_1/\{1\}}\bar{v}^s_{q0}, \tag{93}$$

where $1\le i\le N$. From (92) and (93), $\sum_{q\in\, \mathrm{r}_1}\bar{v}^s_{q0}$ can be obtained as

$$\left[\left(1-\bar{s}\right)\left(\rho-\bar{s}\right)-\rho_{-1}\right]\sum_{q\in\, \mathrm{r}_1}\bar{v}^s_{q0} = \frac{\rho_1\left(1-\bar{s}\right)\sum_{q\in\, \mathrm{r}_1\cup\, \mathrm{r}_2/\{1\}}\bar{\pi}_q}{1+\rho_1-\bar{s}} + \left(\rho_1-\rho\bar{s}\right)\bar{v}^s_{10}. \tag{94}$$

Hence, the MGF of AoI of source 1 can be evaluated as

$$\overset{\text{SA}}{M}_1(\bar{s}) = \sum_{q\in\, \mathcal{Q}}\bar{v}^s_{q0} \overset{\text{(a)}}{=} \frac{(\lambda+\mu-s)\sum_{q\in\, \mathrm{r}_1}\bar{v}^s_{q0} - \lambda\bar{v}^s_{10}}{\mu-s} \overset{\text{(b)}}{=} \frac{\rho_1\Big[\left(1+\rho-\bar{s}\right)\sum_{q\in \mathrm{r}_1\cup\, \mathrm{r}_2/\{1\}}\bar{\pi}_q + \left(1+\rho_1-\bar{s}\right)\bar{v}^s_{10}\Big]}{\left(1+\rho_1-\bar{s}\right)\Big[\left(1-\bar{s}\right)\left(\rho-\bar{s}\right)-\rho_{-1}\Big]}, \tag{95}$$

where step (a) [step (b)] follows from substituting (93) [(94)] into (95). Finally, $\bar{v}^s_{10}$ in (40) can be obtained by following similar steps as in (77)-(79). ■

G. Expressions of AoI Second Moments When $B = 2$

Corollary 9. *When $B = 2$, the first and second moments of AoI of source 1 under the LCFS-WP queueing discipline can be respectively expressed as*

$$\overset{\text{WP}}{\Delta}_{1,1} = \begin{cases} \dfrac{\rho_1^2 + 4\rho_1\rho^3 + 2\rho_{-1}\rho + \rho^2\left(4\rho^4 + 12\rho + 7\right)}{2\mu\rho_1\rho^2\left(3 + 2\rho\right)}, & \text{if } \rho = \beta, \\ \dfrac{\sum_{n=0}^{5}\beta^n\gamma_n}{\mu\rho_1\beta\left(\beta+\rho\right)^2\left[\rho^2 + \beta\left(1+\rho\right)\left(\beta+\rho\right)\right]}, & \text{otherwise.} \end{cases} \tag{96}$$

$$\gamma_5 = \rho_1\rho + \left(1+\rho\right)^2,\ \gamma_4 = 3\rho_1\rho^2 + 3\rho\left(1+\rho\right)^2,\ \gamma_3 = \rho_1^2 + \rho_1\rho\left(3\rho^2 - 2\right) + \rho^2\left(1+\rho\right)\left(5+3\rho\right),$$
$$\gamma_2 = \rho_1^2\rho + \rho_1\rho^2\left(\rho^2 - 2\right) + \rho^3\left(1+\rho\right)\left(5+\rho\right),\ \gamma_1 = \rho^4\left(3+2\rho\right),\ \gamma_0 = \rho^5,$$

$$\overset{\text{WP}}{\Delta}_{1,2} = \begin{cases} \dfrac{2\rho_1^3\left(1+\rho\right) + \rho_1^2\rho\left(8\rho^3 + 2\rho + 3\right) + 8\rho_1\rho^5 + 2\rho_{-1}\rho^2\left(6 + 13\rho\right) + \zeta_0}{2\mu^2\rho_1^2\rho^3\left(3+2\rho\right)}, & \text{if } \rho = \beta, \\ \dfrac{2\sum_{n=0}^{7}\beta^n\psi_n}{\mu^2\rho_1^2\beta^2\left(\beta+\rho\right)^3\left[\rho^2 + \beta\left(1+\rho\right)\left(\beta+\rho\right)\right]}, & \text{otherwise,} \end{cases} \tag{97}$$

$$\zeta_0 = \rho^3\left(8\rho^3 + 36\rho^2 + 28\rho + 15\right),\ \psi_7 = \rho_1^2\rho + \rho_1\left(\rho^2 - 1\right) + \left(1+\rho\right)^3,\ \psi_6 = 4\rho_1^2\rho^2 + 4\rho_1\rho\left(\rho^2 - 1\right) + 4\rho\left(1+\rho\right)^3,$$
$$\psi_5 = \rho_1^3 + \rho_1^2\left(6\rho^3 + \rho + 2\right) + 2\rho_1\rho\left(3\rho^3 - 6\rho - 2\right) + 3\rho^2\left(1+\rho\right)^2\left(3+2\rho\right),$$
$$\psi_4 = 2\rho_1^3\left(1+\rho\right) + \rho_1^2\rho\left(4\rho^3 + 2\rho + 1\right) + 2\rho_1\rho^2\left(2\rho^3 - 9\rho - 4\right) + \rho^3\left(1+\rho\right)^2\left(13 + 4\rho\right),$$
$$\psi_3 = \rho_1^3\rho\left(2+\rho\right) + \rho_1^2\rho^2\left(\rho^3 + \rho + 1\right) + \rho_1\rho^3\left(\rho^3 - 12\rho - 8\right) + \rho^4\left(\rho^3 + 12\rho^2 + 24\rho + 13\right),$$
$$\psi_2 = 2\rho_1^2\rho^3 - 4\rho_1\rho^4\left(1+\rho\right) + 3\rho^5\left(1+\rho\right)\left(3+\rho\right),\ \psi_1 = \rho^6\left(4+3\rho\right) - \rho_1\rho^6,\ \psi_0 = \rho^7.$$

Proof: The expressions in (96) and (97) follow from the fact that the expression of $\overset{\text{WP}}{M}_1(\bar{s})$ (derived in Theorem 4) can be used to compute the k-th moment of AoI of source 1 (denoted by $\overset{\text{WP}}{\Delta}_{1,k}$) as follows

$$\overset{\text{WP}}{\Delta}_{1,k} = \frac{1}{\mu^k} \times \frac{\mathrm{d}^k\left[\overset{\text{WP}}{M}_1(\bar{s})\right]}{\mathrm{d}\bar{s}^k}\Big|_{\bar{s}=0}, \tag{98}$$

where $\frac{\mathrm{d}^k}{\mathrm{d}\bar{s}^k}$ denotes the k-th derivative with respect to $\bar{s}$. ■

Corollary 10. *When $B = 2$, the first and second moments of AoI of source 1 under the LCFS-PS queueing discipline can be respectively expressed as*

$$\overset{\text{PS}}{\Delta}_{1,1} = \begin{cases} \dfrac{\rho_1^2\left(1+\rho\right) + 2\rho_{-1}\rho\left(\rho^2 + \rho + 1\right) + \rho^2\left(4\rho^3 + 14\rho^2 + 19\rho + 7\right)}{2\mu\rho_1\rho^2\left(1+\rho\right)\left(3+2\rho\right)}, & \text{if } \rho = \beta, \\ \dfrac{\sum_{n=0}^{5}\beta^n\gamma'_n}{\mu\rho_1\beta\left(1+\rho\right)\left(\beta+\rho\right)^2\left[\rho^2 + \beta\left(1+\rho\right)\left(\beta+\rho\right)\right]}, & \text{otherwise.} \end{cases} \tag{99}$$

$$\gamma'_5 = \left(1+\rho\right)^3,\ \gamma'_4 = 3\rho\left(1+\rho\right)^3,\ \gamma'_3 = \rho_1^2\left(1+\rho\right) - \rho_1\rho\left(\rho^2 + 2\rho + 2\right) + \rho^2\left(1+\rho\right)^2\left(5+3\rho\right),$$
$$\gamma'_2 = \rho_1^2\rho\left(1+\rho\right) - 2\rho_1\rho^2\left(\rho^2 + \rho + 1\right) + \rho^3\left(1+\rho\right)^2\left(5+\rho\right),\ \gamma'_1 = \rho^4\left(1+\rho\right)\left(3+2\rho\right) - \rho_1\rho^5,\ \gamma'_0 = \rho^5\left(1+\rho\right),$$

$$\overset{\text{PS}}{\Delta}_{1,2} = \begin{cases} \dfrac{2\rho_1^3\left(1+\rho\right)\left(1+2\rho\right) + \rho_1^2\rho\left(2\rho^3 + 11\rho^2 + 8\rho + 3\right) + \rho_{-1}\zeta'_1 + \zeta'_0}{2\mu^2\rho_1^2\rho^3\left(1+\rho\right)^2\left(3+2\rho\right)}, & \text{if } \rho = \beta, \\ \dfrac{2\sum_{n=0}^{7}\beta^n\psi'_n}{\mu^2\rho_1^2\beta^2\left(\beta+\rho\right)^3\left(1+\rho\right)^2\left[\rho^2 + \beta\left(1+\rho\right)\left(\beta+\rho\right)\right]}, & \text{otherwise,} \end{cases} \tag{100}$$

$$\zeta_1' = 2\rho^2(1+\rho)\left(8\rho^3+22\rho^2+19\rho+6\right),\ \zeta_0' = \rho^3(1+\rho)(3+2\rho)\left(4\rho^3+8\rho^2+11\rho+5\right),$$
$$\psi_7' = (1+\rho)^5 - \rho_1(1+\rho)^3,\ \psi_6' = 4\rho(1+\rho)^5 - 4\rho_1\rho(1+\rho)^3,$$
$$\psi_5' = \rho_1^3(1+\rho) + \rho_1^2\left(2\rho^3+6\rho^2+5\rho+2\right) - 4\rho_1\rho(1+\rho)\left(2\rho^3+5\rho^2+4\rho+1\right) + 3\rho^2(1+\rho)^4(3+2\rho),$$
$$\psi_4' = 2\rho_1^3(1+\rho)(1+2\rho) + \rho_1^2\rho\left(3\rho^3+9\rho^2+4\rho+1\right) - 2\rho_1\rho^2(1+\rho)\left(5\rho^3+14\rho^2+13\rho+4\right)$$
$$+\rho^3(1+\rho)^2\left(4\rho^3+21\rho^2+30\rho+13\right),$$
$$\psi_3' = \rho_1^3\rho(1+\rho)(2+3\rho) + \rho_1^2\rho^2\left(5\rho^2+3\rho+1\right) - \rho_1\rho^3(1+\rho)\left(7\rho^3+20\rho^2+20\rho+8\right)$$
$$+\rho^4(1+\rho)^2\left(\rho^3+12\rho^2+24\rho+13\right),$$
$$\psi_2' = \rho_1^2\rho^3\left(-\rho^3+2\rho^2+4\rho+2\right) - 2\rho_1\rho^4(1+\rho)\left(\rho^3+4\rho^2+4\rho+2\right) + 3\rho^5(1+\rho)^3(3+\rho),$$
$$\psi_1' = \rho^6(1+\rho)^2(4+3\rho) - \rho_1\rho^6(1+\rho)(1+2\rho),\ \psi_0' = \rho^7(1+\rho)^2.$$

Corollary 11. *When $B=2$, the first and second moments of AoI of source 1 under the LCFS-SA queueing discipline can be respectively expressed as*

$$\overset{\text{SA}}{\Delta}_{1,1} = \begin{cases} \dfrac{\rho_1^3+\rho_1^2+\rho_1\rho^2\left(4\rho^2+10\rho+7\right)+\rho^2\left(4\rho^2+12\rho+5\right)+2\rho_{-1}\rho\left[\rho_1(3\rho+1)+2\right]}{2\mu\rho_1\rho^2(1+\rho_1)(3+2\rho)}, & \text{if } \rho=\beta, \\ \dfrac{\sum_{n=0}^{5}\beta^n\bar{\gamma}_n}{\mu\rho_1\beta(1+\rho_1)(\beta+\rho)^2\left[\rho^2+\beta(1+\rho)(\beta+\rho)\right]}, & \text{otherwise.} \end{cases} \tag{101}$$

$$\bar{\gamma}_5 = -\rho_1^2+\rho_1\left(\rho^2+3\rho+1\right)+(1+\rho)^2,\ \bar{\gamma}_4 = -3\rho_1^2\rho+3\rho_1\rho\left(\rho^2+3\rho+1\right)+3\rho(1+\rho)^2,$$
$$\bar{\gamma}_3 = \rho_1^3+\rho_1^2\left(-4\rho^2-2\rho+1\right)+\rho_1\rho\left(3\rho^3+11\rho^2+5\rho-2\right)+\rho^2(1+\rho)(5+3\rho),$$
$$\bar{\gamma}_2 = \rho_1^3\rho-\rho_1^2\rho(1+\rho)(3\rho-1)+\rho_1\rho^2\left(\rho^3+7\rho^2+5\rho-2\right)+\rho^3(1+\rho)(5+\rho),$$
$$\bar{\gamma}_1 = -\rho_1^2\rho^4+\rho^4(2\rho+3)(1+\rho_1),\ \bar{\gamma}_0 = \rho^5(1+\rho_1),$$

$$\overset{\text{SA}}{\Delta}_{1,2} = \begin{cases} \dfrac{\sum_{n=0}^{5}\rho_1^n\bar{\zeta}_n+\rho_{-1}\rho_1^2\bar{\zeta}_6+\rho_{-1}^2\rho_1\bar{\zeta}_7+\rho_{-1}\rho_1\bar{\zeta}_8+\rho_{-1}\bar{\zeta}_9}{2\mu^2\rho_1^2\rho^3(1+\rho_1)^2(3+2\rho)}, & \text{if } \rho=\beta, \\ \dfrac{2\sum_{n=0}^{7}\beta^n\bar{\psi}_n}{\mu^2\rho_1^2\beta^2(\beta+\rho)^3(1+\rho_1)^2\left[\rho^2+\beta(1+\rho)(\beta+\rho)\right]}, & \text{otherwise,} \end{cases} \tag{102}$$

$$\bar{\zeta}_9 = 12\rho^2,\ \bar{\zeta}_8 = \rho^2(43\rho+22),\ \bar{\zeta}_7 = \rho^2(18\rho+4),\ \bar{\zeta}_6 = \rho^2\left(24\rho^2+74\rho+8\right),\ \bar{\zeta}_5 = 2,\ \bar{\zeta}_4 = 6\rho^2+5\rho+4,\ \bar{\zeta}_3 = 2(4\rho+1),$$
$$\bar{\zeta}_2 = \rho\left(8\rho^5+20\rho^4+3\right),\ \bar{\zeta}_1 = \rho^3\left(16\rho^3+62\rho^2+61\rho+6\right),\ \bar{\zeta}_0 = \rho^3\left(8\rho^3+36\rho^2+54\rho+15\right),$$
$$\bar{\psi}_7 = -\rho_1^3(3+2\rho)+\rho_1^2\left(\rho^3+4\rho^2+2\rho-2\right)+\rho_1(1+\rho)\left(2\rho^2+5\rho+1\right)+(1+\rho)^3,$$
$$\bar{\psi}_6 = -4\rho_1^3\rho(3+2\rho)+4\rho_1^2\rho\left(\rho^3+4\rho^2+2\rho-2\right)+4\rho_1\rho(1+\rho)\left(2\rho^2+5\rho+1\right)+4\rho(1+\rho)^3,$$
$$\bar{\psi}_5 = 3\rho_1^4(1+\rho)-\rho_1^3\left(14\rho^3+27\rho^2-5\right)+\rho_1^2\left(6\rho^5+27\rho^4+16\rho^3-23\rho^2-7\rho+2\right)+2\rho_1\rho\left(6\rho^4+24\rho^3+24\rho^2+3\rho-2\right)$$
$$+3\rho^2(3+2\rho)(1+\rho)^2,$$
$$\bar{\psi}_4 = 2\rho_1^5+\rho_1^4\left(6\rho^2+3\rho+4\right)-\rho_1^3\left(14\rho^4+35\rho^3-4\rho-2\right)+\rho_1^2\rho\left(4\rho^5+25\rho^4+20\rho^3-33\rho^2-14\rho+1\right)$$
$$+2\rho_1\rho^2\left(4\rho^4+23\rho^3+30\rho^2+4\rho-4\right)+\rho^3(13+4\rho)(1+\rho)^2,$$
$$\bar{\psi}_3 = 2\rho_1^5\rho+\rho_1^4\rho\left(3\rho^2+2\rho+4\right)-\rho_1^3\rho\left(8\rho^4+24\rho^3+4\rho^2-3\rho-2\right)+\rho_1^2\rho^2\left(\rho^5+13\rho^4+17\rho^3-19\rho^2-15\rho+1\right)$$
$$+\rho_1\rho^3\left(2\rho^4+25\rho^3+48\rho^2+14\rho-8\right)+\rho^4(1+\rho)\left(\rho^2+11\rho+13\right),$$
$$\bar{\psi}_2 = 2\rho_1^4\rho^3-\rho_1^3\rho^3\left(2\rho^3+9\rho^2+4\rho-4\right)+\rho_1^2\rho^3\left(3\rho^4+10\rho^3-3\rho^2-8\rho+2\right)+2\rho_1\rho^4\left(3\rho^3+12\rho^2+7\rho-2\right)$$
$$+3\rho^5(1+\rho)(3+\rho),$$
$$\bar{\psi}_1 = -2\rho_1^3\rho^6+\rho_1^2\rho^6(1+3\rho)+\rho_1\rho^6(7+6\rho)+\rho^6(4+3\rho),\ \bar{\psi}_0 = \rho^7(1+\rho_1)^2.$$